Tumors of the Mesentery and Omentum

Hoon Ji, Pablo R. Ros

4.11

Contents

Introduction

Cross-sectional imaging techniques (ultrasound (US), computed tomography (CT) and magnetic resonance imaging (MRI)) will depict abdominal lesions in the connecting folds of tissue that constitute the mesentery (including small bowel mesentery, mesocolon, mesosigmoid and mesoappendix) and omentum (including both greater omentum or epiploon) and lesser omentum or gastrohepatic ligament. All of these folds of tissue are covered by peritoneum.

Although uncommon, mesenteric/omental tumors are encountered in all age groups from infancy to the very elderly. These tumors should be considered as possible causes for a palpable abdominal mass, but they are most commonly brought into the differential diagnosis of abdominal pathology once discovered by a radiologic study. An increased awareness of both neoplastic and non-neoplastic processes resulting in mesenteric masses aids the clinical radiologist in differentiating these diseases.

Cross-sectional imaging techniques are able to clearly depict mesenteric and omental masses and determine if they are cystic or solid. To make this determination, a practical approach involving both cystic and solid patterns is used, highlighting the radiologic-pathologic features that may allow a specific diagnosis.

Cystic Masses

Once it is determined that a cystic abdominal mass arises from the mesentery or omentum rather than a solid abdominal organ, the differential diagnosis includes primary mesenteric/omental cyst, mesenteric teratoma, cystic mesothelioma, cystic spindle cell tumor (cystic leiomyoma/leiomyosarcoma), pseudomyxoma peritonei, pancreatic pseudocyst, mycobacterium avium-intracellulare (MAI) adenopathy and complicated ascites (Table 1) [1, 2].

Mesenteric/Omental Cysts

Mesenteric/omental cysts are rare: the incidence is about 1 per 140,000 general hospital admissions and about 1 per 20,000 pediatric hospital admissions [3–5]. In a study from Egleston Children's Hospital at Emory University from 1965–1994, 14 patients were treated for mesenteric or omental cysts, which represents a prevalence of about 1 case per 11,250 admissions [6]. Approximately one third of cases occur in children younger than 15 [7]. Mesenteric cysts are 4.5 times more common than omental cysts [8].

A classification of mesenteric/omental cysts based essentially on histopathological features should include the following six groups: (1) cysts of lymphatic origin (simple lymphatic cyst and lymphangioma); (2) cysts of enteric origin (enteric cyst and enteric duplication cyst); (3) cysts of mesothelial origin (simple mesothelial cyst, benign cystic mesothelioma, and malignant cystic mesothelioma); (4) cysts of urogenital origin; (5) mature cystic teratoma (dermoid cysts), and (6) pseudocysts (infectious and traumatic cysts) (Table 2).

Table 1. Mesenteric/Omental Cystic Masses[a]

I.	Mesenteric/Omental Cyst
	Lymphangioma
	Enteric duplication cyst
	Enteric cyst
	Mesothelial cyst
	Nonpancreatic pseudocyst
II.	Neoplasms
	Teratoma
	Cystic mesothelioma
	Cystic spindle cell tumor (leiomyoma/leiomyosarcoma)
	Pseudomyxoma peritonei
III.	Miscellaneous
	Pancreatic pseudocyst
	MAI adenopathy
	Complicated ascites

[a] Modified from references 1 and 10

Table 2. Histologic Classification of Mesenteric/Omental Cysts[a]

Diagnosis	Histologic Features
Lymphangioma	Endothelial lining
Enteric duplication cyst	Enteric lining, double muscle layer with neural elements
Enteric cyst	Enteric lining, no muscle layer
Mesothelial cyst	Mesothelial lining
Pseudocyst (nonpancreatic)	No lining, fibrous wall

[a] From reference 3

Lymphangioma

Lymphangioma is the most common subtype of mesenteric/omental cyst and represents a congenital malformation of the lymphatic vessels arising from the bowel [4]. Ninety-five percent of lymphangiomas are found in the neck and axilla [9]. In cases with the mesenteric/omental lymphangioma, abdominal distention with a palpable mass is the most common clinical presentation [10].

Pathologic Findings

Lymphangiomas are large, thin-walled multiloculated cystic masses lined with endothelium (Fig. 1). The contents may be chylous or hemorrhagic. Prominent stromal myxoid degeneration may occur rarely [11]. Lymphangiomas are intimally attached to the bowel wall and are the only type of mesenteric/omental cyst that routinely requires bowel resection for removal [10].

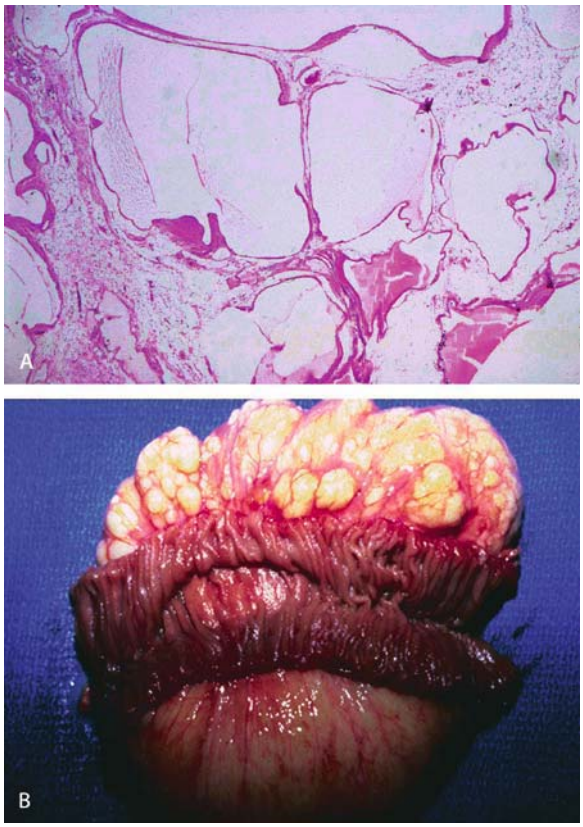

Fig. 1A, B. Lymphangioma: pathology. **A** Photomicrograph demonstrates a typical lymphangioma consisting of multiloculated cystic lesion with endothelial cell lining. **B** Resected specimen shows the large mass intimately attached to bowel

Imaging Features

Plain radiograph and barium studies may demonstrate a small bowel obstruction (frequently partial) and possibly a noncalcified soft-tissue mass or displaced bowel loops [10]. US demonstrates lymphangiomas to be anechoic, multiseptate masses (Fig. 2). On CT, they are multiloculated, frequently seen surrounding or tethered by a loop of bowel from where they originate and with Hounsfield units ranging from water (if the contents are serous) to fat (if the contents are chylous) attenuation [12]. CT allows differentiation of lymphangioma from ascites with separation of bowel loops, absence of fluid

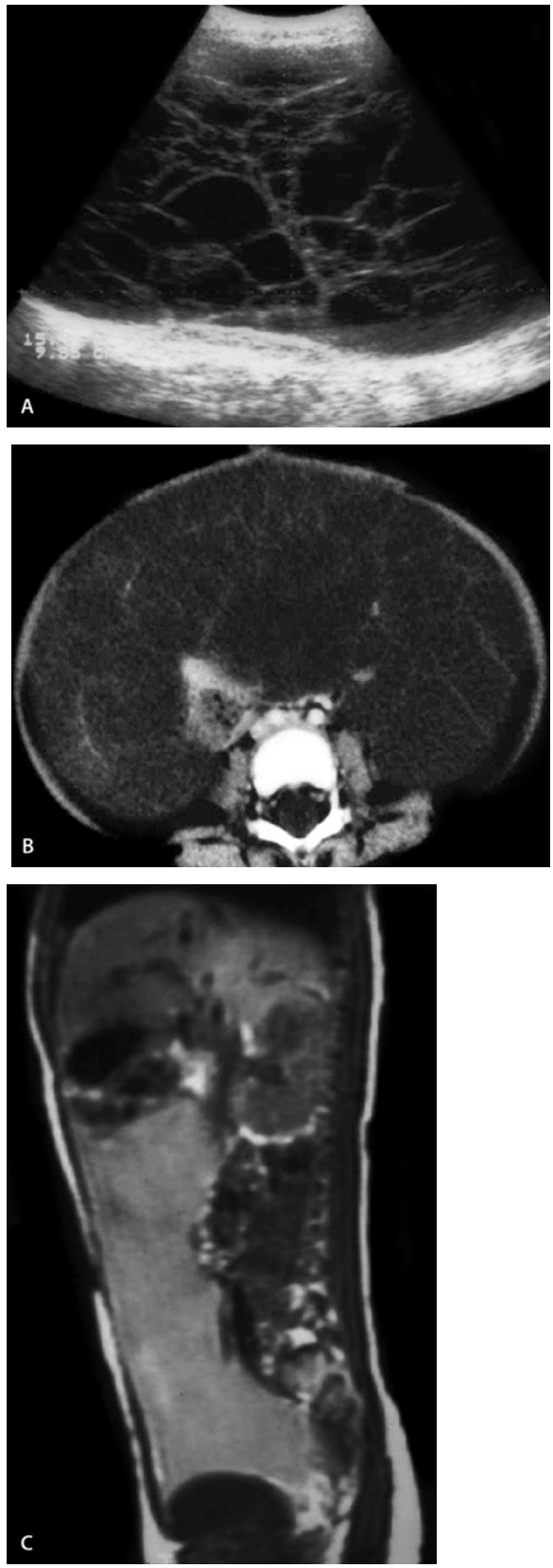

Fig. 2A–C. Lymphangioma: imaging features. **A** Ultrasonogram (US) demonstrates a large multilocular cystic mass in abdomen. **B** Enhanced CT scan of the abdomen demonstrates a multilocular cystic mass containing fluid of water attenuation. **C** T1-weighted MR image of the entire abdomen in the sagittal plane demonstrates a large mass centered in the mesentery. The high-intensity of the fluid corresponds to the fat seen in the chylous material typically contained in lymphangiomas

in the perihepatic spaces and cul-de-sac, and focal septations [13]. MRI is helpful to characterize the chylous (fatty nature) of the contents due to high signal intensity in T1-weighted images [14].

Enteric Duplication Cyst

Duplications of the alimentary tract are uncommon congenital abnormalities. When an enteric duplication (usually attached to the bowel) migrates into the mesentery, it becomes a mesenteric cyst [10]. Duplications are usually observed early in life, but a minority remains unsuspected until adulthood [15]. The clinical presentation may depend on the location of the duplication and adjacent structures, and includes abdominal distention, vomiting, bleeding, and a palpable abdominal mass. The symptoms and signs produced by duplications, however, are often vague [16]. Complications such as perforation, intussusception, volvulus, and associated malignancy may occur [17].

Pathologic Findings

Enteric duplication cysts are usually small, thick-walled and unilocular with predominantly serous contents. The wall "reduplicates" the normal wall of the bowel and contains all layers, including mucosa, circular and longitudinal muscular layers and mesenteric plexus (Fig. 3). Gastric mucosa can be present in 17%–36% of duplication cysts [18–20], and which may cause gastrointestinal bleeding.

Imaging Features

By US, enteric duplication cysts have a thick wall similar in composition to the normal bowel wall. It contains multiple layers, typically including an echogenic inner mucosal layer and a hypoechoic outer muscular layer (Fig. 4). Enteric duplication cysts containing gastric mucosa may be demonstrated with uptake of technetium-

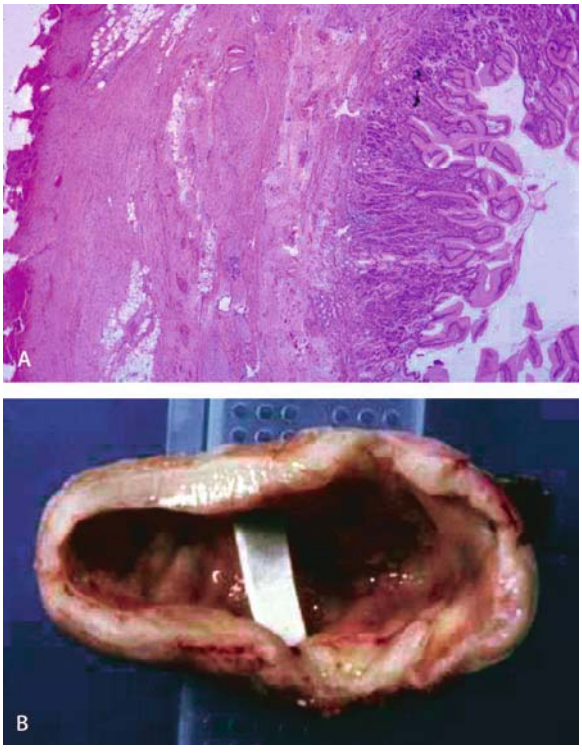

Fig. 3A, B. Enteric duplication cyst: pathology. **A** Photomicrograph demonstrates a typical enteric duplication cyst with thick wall lined by enteric epithelium. **B** Gross specimen shows a thick-walled unilocular cystic mass with serous contents

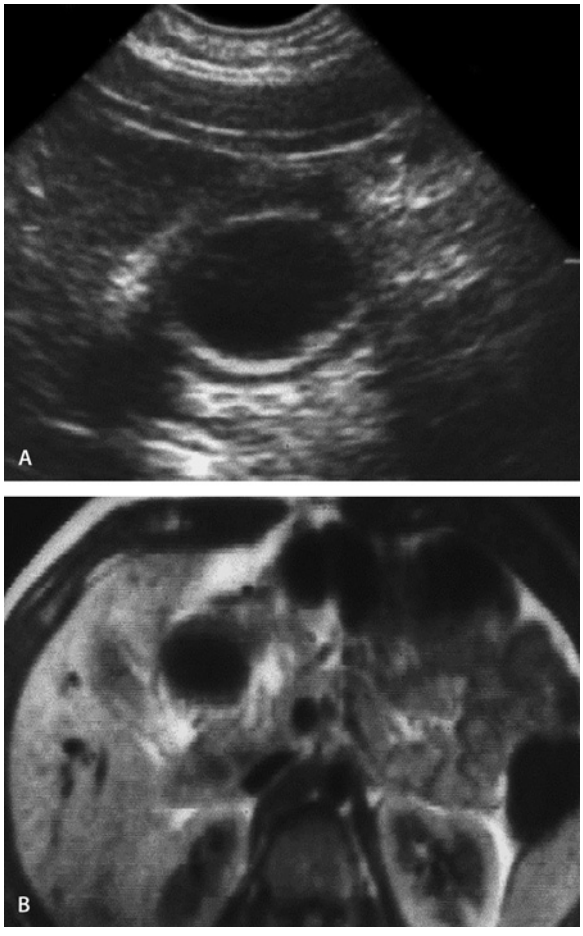

Fig. 4A, B. Enteric duplication cyst: imaging features. **A** US demonstrates a small unilocular cystic lesion with multilayered wall. **B** Axial T1-weighted MR image demonstrates a low signal intensity lesion with thick wall (*arrow*)

99m sodium pertechnetate [19]. CT and MRI reveal a cystic mass in the mesentery with a thick wall that enhances after administration of contrast material. Attenuation of the lesion on CT scans may be high due to the mucoid-rich viscous fluid within the cyst [1, 20].

Enteric Cyst

Enteric cysts are lined with enteric (gastrointestinal tract) mucosa, and have a thin fibrous wall (without reduplication of the bowel wall as in enteric duplication cysts) [10, 21]. They are usually unilocular with serous contents and a thin, smooth wall that cannot be visualized by CT or MRI [1, 10] (Fig. 5).

Mesothelial Cyst

Mesothelial cysts are the rarest type of mesenteric/omental cyst and are the result of a failure in the coalescence of the mesothelially lined peritoneal surfaces [10]. The reported incidence varies between 1 in 30,000 and 1 in 200,000 admissions [22]. Clinical presentation includes an asymptomatic abdominal mass, vague chronic abdominal complains, nausea, vomiting or diarrhea [23].

Pathologic Findings

Mesothelial cysts are thin-walled with a characteristic mesothelial lining of the inner surface (Fig. 6). Although they may occur in the mesentery, they are more common in the greater omentum and mesocolon [4, 10].

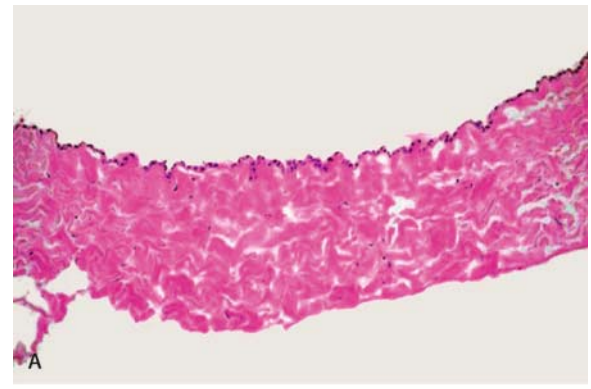

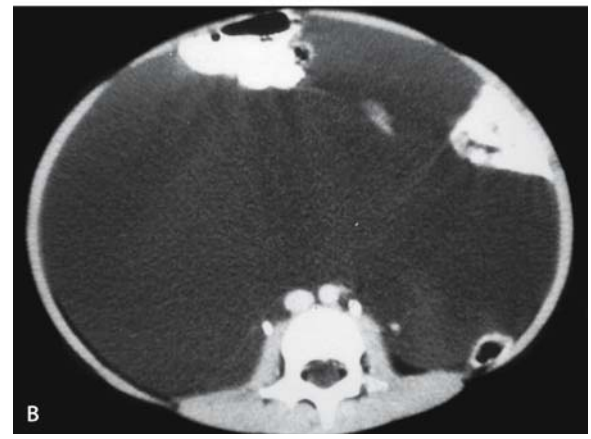

Fig. 6A, B. Mesothelial cyst. **A** Photomicrograph demonstrates a thin-walled cystic mass with mesothelial lining of the inner surface. **B** CT scan shows a large cystic mass displacing bowel loops

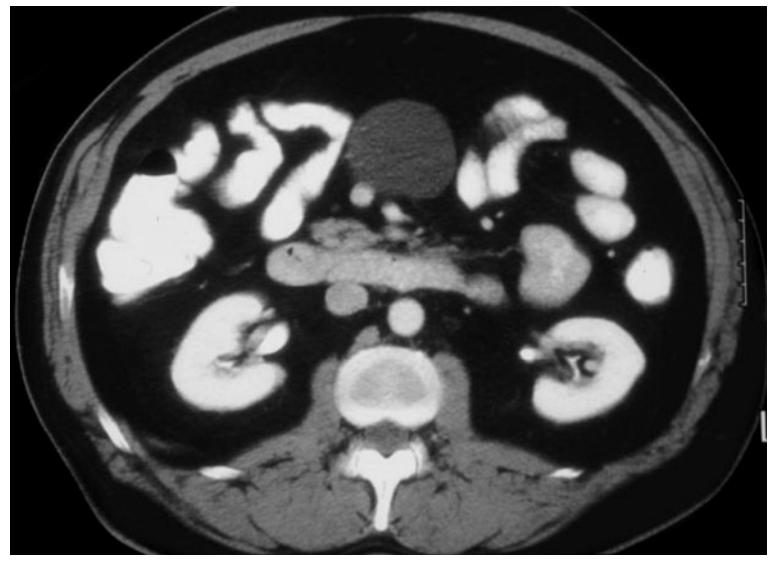

Fig. 5. Enteric cyst: CT appearance. A well-defined cystic mass with attenuation in the range of water is seen in the mesentery, near the superior mesenteric vessels. Note that the wall is not perceptible by CT

Imaging Features

US and CT demonstrate unilocular, thin-walled cystic mass (Fig. 6). They are indistinguishable radiologically from enteric cysts [1, 10, 22].

Nonpancreatic Pseudocyst

By definition, nonpancreatic pseudocysts have no inner cellular lining and are thought to be the sequelae of either a mesenteric/omental hematoma or abscess [10].

Pathologic Findings

They are thick-walled cystic masses with no lining epithelium, usually septate and contain hemorrhagic or purulent debris.

Imaging Features

Radiologically, nonpancreatic pseudocysts have a thick wall and may contain fluid-fluid levels corresponding to hemorrhagic or purulent contents [1, 10] (Fig. 7).

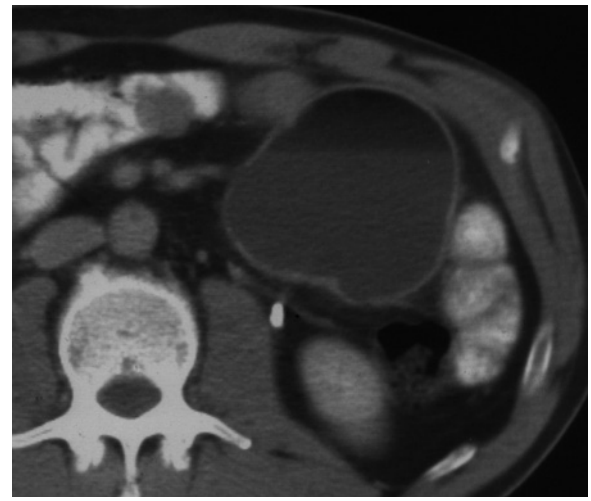

Fig. 7. Nonpancreatic pseudocyst, CT appearance. Enhanced CT of the abdomen demonstrates a thick-walled cystic mass with a fluid-fluid level, typical of pseudocyst containing hemorrhagic debris

Teratoma

This uncommon benign cystic neoplasm of the mesentery or omentum occurs primarily in infancy or childhood but rarely in adult [24–26]. Implantation of ovarian teratoma in the mesentery or omentum has been proposed for an explanation of its pathogenesis [27]. Clinical presentation is usually a palpable mass with associated manifestations, depending on its location.

Pathologic Findings

Grossly, teratomas of the mesentery/omentum are predominantly cystic with solid areas that contain fat or calcification. Histologic components include three germinal layer elements such as skin appendages, cartilage, bone, adipose tissue, and glial/glandular tissue [10, 24] (Fig. 8).

Imaging Features

Radiographically, calcifications are frequently present. Sonography reliably demonstrates the mixed cystic and solid nature of the teratoma (Fig. 9). The cystic component shows an anechoic area in the tumor. The solid

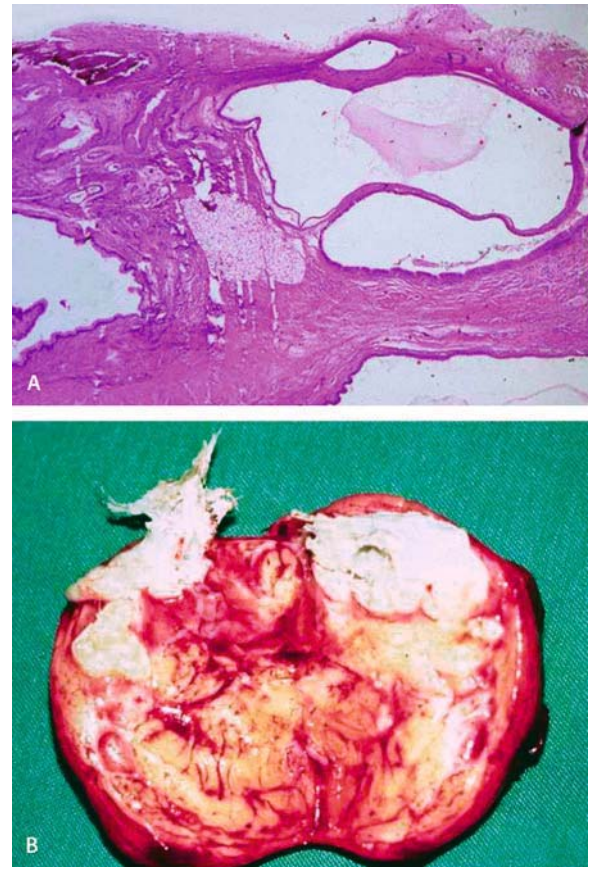

Fig. 8A, B. Mesenteric teratoma, pathologic findings. **A** Photomicrograph demonstrates a typical teratoma consisting of cartilage, skin appendages, and fat. **B** Gross specimen shows a well-demarcated cystic mass with heterogeneous internal contents

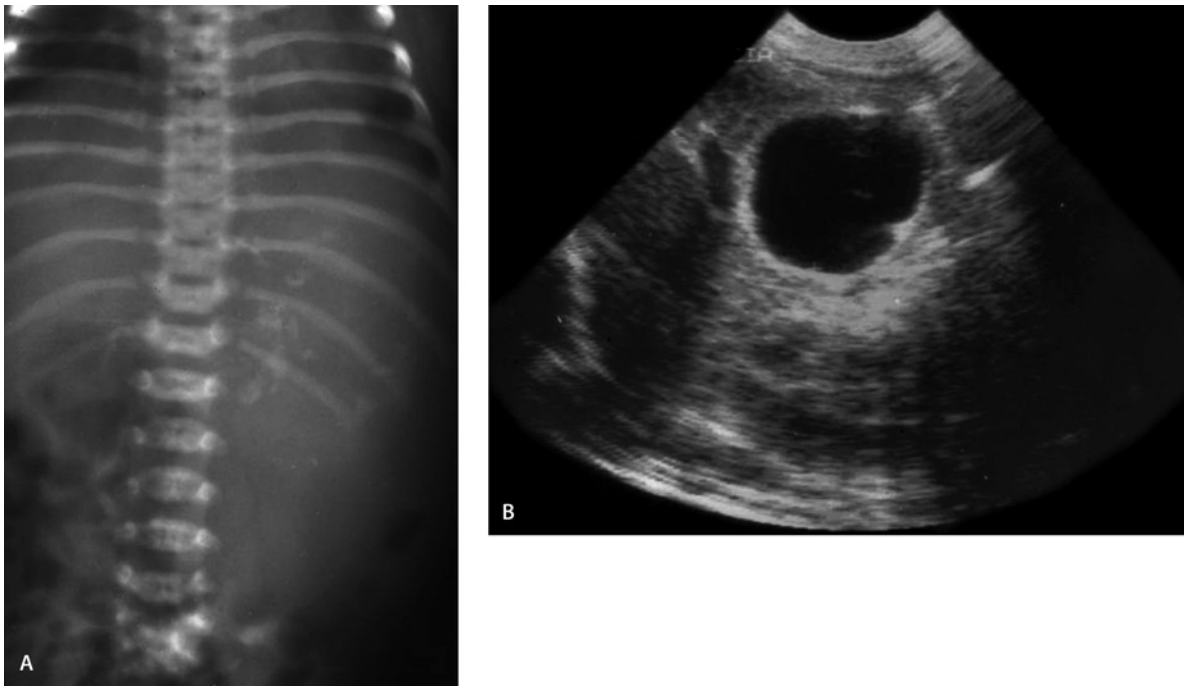

Fig. 9A, B. Mesenteric teratoma, plain film and US findings. **A** Supine film of the abdomen in an infant demonstrates multiple dystrophic calcifications in the left upper quadrant. **B** US shows a well-demarcated mass and cystic nature of the lesion

component shows homogeneous moderate-intensity echoes, and sometimes even higher echogenic areas characteristic of fat and calcification [24]. CT demonstrates a predominantly cystic tumor with attenuation in the range of water except for peripheral areas in the fat attenuation range [24, 26] (Fig. 10). Calcifications may be identifiable as well.

Cystic Mesothelioma

Cystic mesothelioma is a rare benign neoplasm of the peritoneum, unrelated to malignant peritoneal mesothelioma. Cystic mesothelioma is not a malignant mesothelioma that has undergone necrosis and cystic transformation. It is unrelated to asbestos exposure [2]. Cystic

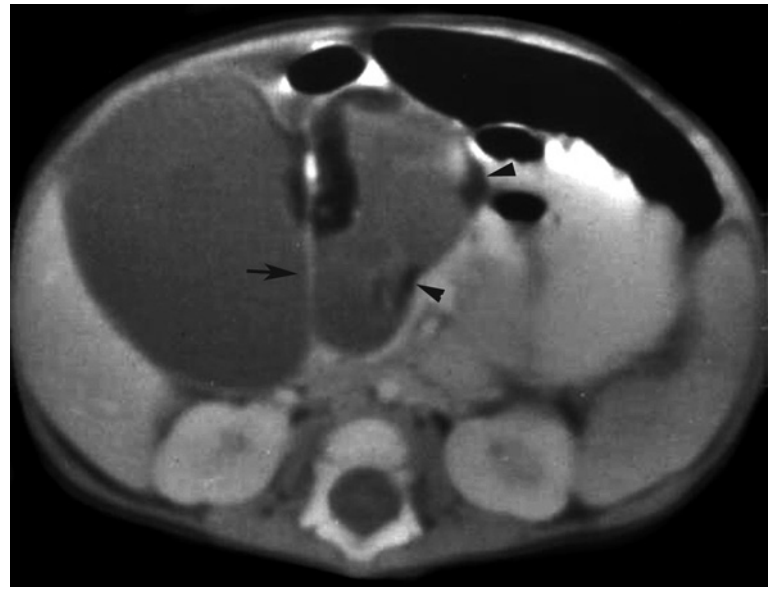

Fig. 10. Teratoma of the lesser omentum, CT appearance. A bilobed cystic mass is seen with attenuation in the range of water. A focus of calcification is seen in the central septation (*arrow*). Areas of fat are seen peripherally (*arrowheads*)

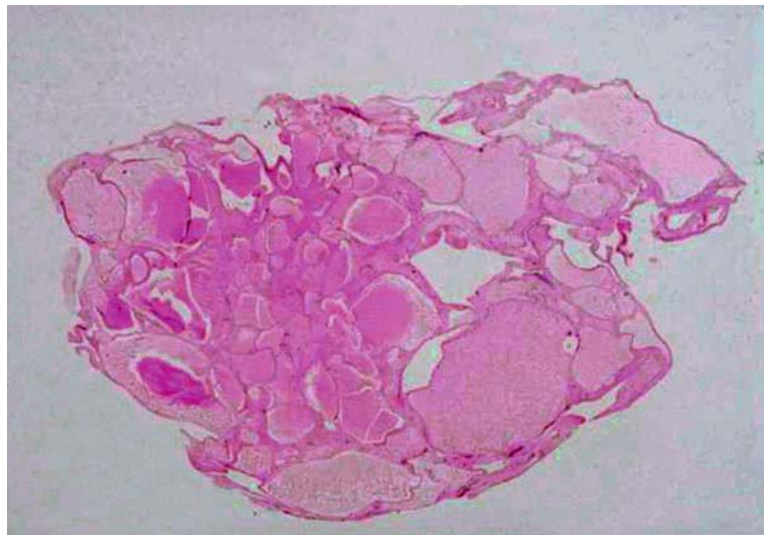

Fig. 11. Cystic mesothelioma, pathologic finding. Photomicrograph demonstrates typical findings of a cystic mesothelioma composed of mesothelium-lined cysts surrounded by a fibrovascular stroma

mesothelioma is almost always encountered in middle-aged women who present with abdominal pain and/or a palpable mass. It is considered a low-grade malignancy because it recurs locally, although generally it does not metastasize [28]. Although it may involve any peritoneal or omental surface, it is much more frequently seen in the pelvis.

Pathologic Findings

The tumor is composed of multiple cysts, ranging in size from a few millimeters (mm) to six centimeters (cm) and containing clear watery fluid. Histopathologic finding shows multiple mesothelium-lined cysts surrounded by a fibrovascular stroma [29] (Fig. 11).

Imaging Features

By ultrasound, they appear as multiloculated cystic masses, usually large. CT demonstrates a well-defined, non-calcified mass, although a few cases with calcification have been reported [30, 31]. Cystic mesothelioma compresses and surrounds bowel loops, but typically does not cause bowel obstruction (Fig. 12). MRI shows the cystic masses that have hypointensity on T1-weighted images and intermediate or hyper signal on T2-weighted images, correlating with their watery-like contents [1, 32] (Fig. 13).

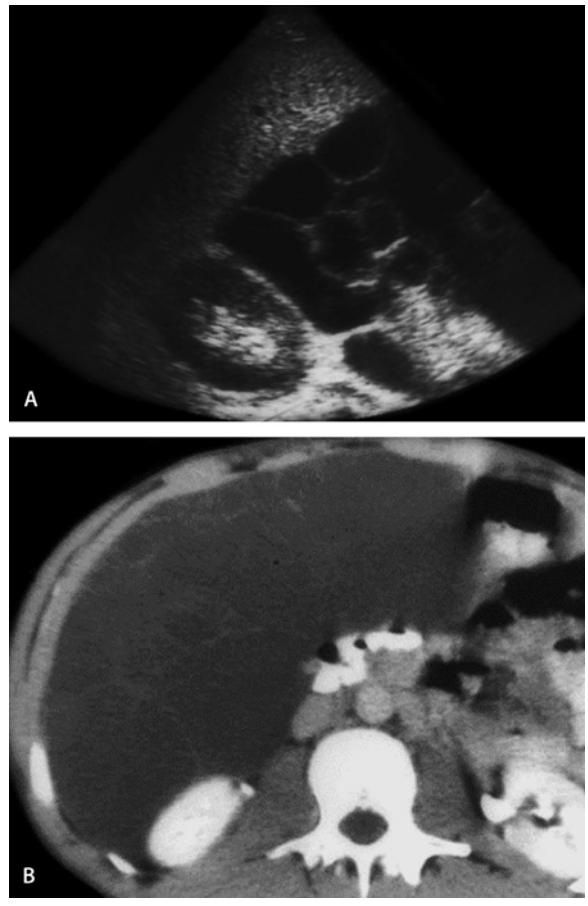

Fig. 12A, B. Cystic mesothelioma, US and CT features. **A** US of the upper abdomen demonstrates a multiple cystic mass with septations. **B** On CT scan, multiple water-density masses are seen in the abdomen, displacing loops of bowel without obstructing them

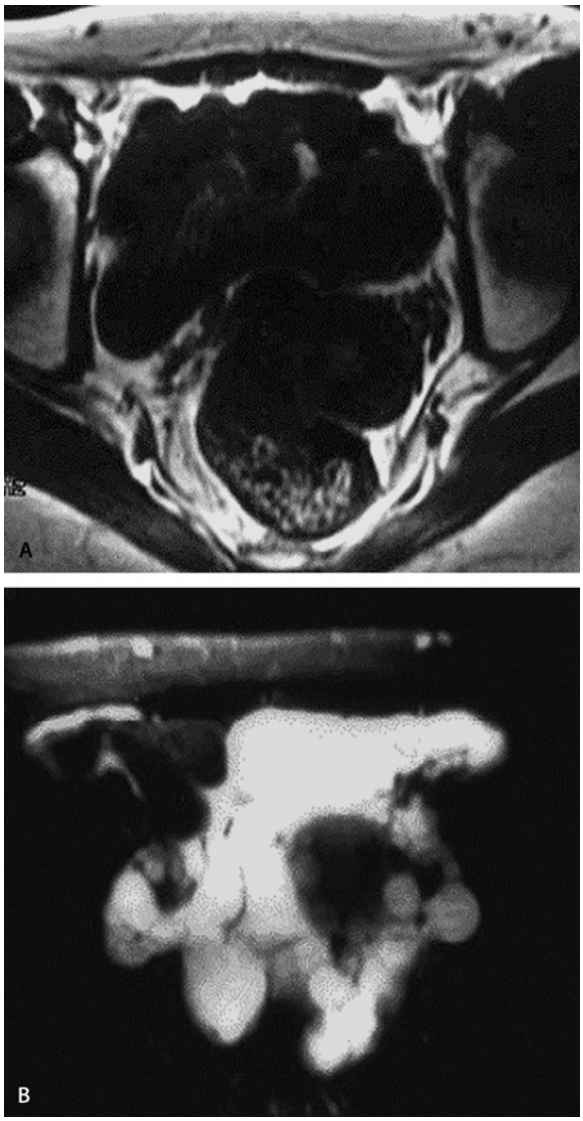

Fig. 13A, B. Cystic mesothelioma, MRI appearance. **A** T1-weighted MR image demonstrates a multilocular low signal intensity lesion in pelvic cavity. **B** T2-weighted MR image shows high signal intensity of the lesion correlating of watery contents

Cystic Spindle Cell Tumor

Spindle cell tumors in the mesentery/omentum and gastrointestinal tract (i.e., gastrointestinal stromal tumor, leiomyoma/leiomyosarcoma, schwannomas) can undergo central liquefactive necrosis and hemorrhage, appearing as complex cystic mesenteric/omental masses on US or CT [1, 33, 34].

Pathologic Findings

Grossly, cystic mesenchymal tumors are large masses with internal debris and hemorrhage. They may invade the surrounding structures such as the bowel or solid abdominal organs. Microscopic examination may reveal foci of myxoid degeneration, microcyst formation epithelioid or spindle cells with prominent cytoplasmic vacuolization. Immunohistochemical studies enable differential diagnosis of subsets of mesenchymal tumors [34, 35].

Imaging Features

US demonstrates a complex mass with large amounts of internal echoes [33] (Fig. 14). By CT, the mass has a low-attenuation central zone surrounded by irregular walls

Fig. 14A, B. Cystic spindle cell tumor (leiomyosarcoma), imaging features. **A** US demonstrates a large complex cystic mass with heterogeneous internal echoes. **B** Axial CT scan shows a large, well-defined cystic mass with solid portion, corresponding to viable portions of the tumor

and a high-attenuation peripheral rim, corresponding to viable tumor [1, 34, 36].

Pseudomyxoma Peritonei

Pseudomyxoma peritonei is defined as massive and diffuse involvement of the peritoneal cavity by a low-grade metastatic mucinous adenocarcinoma originating in the ovary, appendix, or colon. It is most common in women aged between 50–70 [37]. Clinically the main complaints of pseudomyxoma include abdominal pain, abdominal distention, partial bowel obstruction, and fistula formation [38].

Pathologic Findings

Typically pseudomyxoma peritonei manifests as multiple discrete nodules containing mucin on the peritoneum (Fig. 15). It may have solid and hemorrhagic areas and septal calcifications. Microscopically pseudomyxoma nodules are characterized by multifocal pools of mucin with scant strips of mucinous epithelium or varying proportion of glandular and signet ring cell components [1, 2].

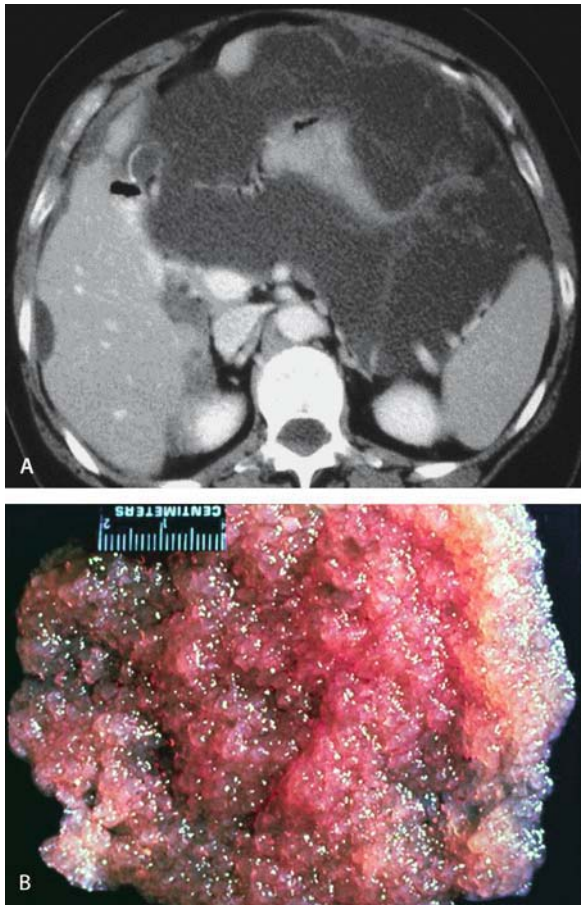

Fig. 15A, B. Pseudomyxoma peritonei. **A** Enhanced CT scan of the abdomen demonstrates multiple cystic masses encasing the stomach and producing scalloping of the liver. **B** Gross specimen shows the multiple discrete nodules containing mucin on the peritoneum

Imaging Features

Ultrasonography is useful to detect hypoechoic cysts or ascites with scalloping of hepatic or splenic margins due to extrinsic pressure of adjacent peritoneal implants [39]. CT scans demonstrates myxomatous tumor collections that are of low attenuation (Fig. 15). Areas of high attenuation or solid component can be seen within it. Calcifications may also be present. Pseudomyxoma peritonei may mimic ascites, but it should not be confused with the latter, Pseudomyxoma peritonei, unlike ascites, produces scalloping of the liver and spleen, as well as encasement with displacement of the gastrointestinal tract [2, 38]. Spread of mucinous material to the pleural cavity may occur, presumably through the congenital pleuroperitoneal communication [40]. MRI may be useful in assessment of small bowel obstruction in patients with pseudomyxoma peritonei [41].

Miscellaneous Cystic Mesenteric/ Omental Lesions

Pancreatic Pseudocyst

Pancreatic pseudocysts are common cystic masses, sequelae of acute pancreatitis. The clinical history, laboratory findings and classic CT appearance are usually diagnostic of this entity.

Mycobacterium avium-intracellulare Adenopathy

Mesenteric adenopathy may have marked low attenuation by CT, mimicking the appearance of multiple cystic masses, such as those caused by infection with *Mycobacterium avium-intracellulare* (MAI) [42].

Pathologic Findings

Multiple conglomerated nodular masses are found in the mesentery and/or omentum, often adherent to bowel and other solid organs. Cross-sectional specimens show that caseous or liquefactive substances in the center of the enlarged lymph nodes are surrounded by inflammatory lymphatic tissue and preserved blood vessels [43].

Imaging Features

MAI lymphadenopathy has extremely low attenuation by CT with an enhancing rim [44]. The anatomic distribution and specific enhancement patterns of lymphadenopathy seen on contrast-enhanced CT or MRI can be useful in differentiating between tuberculosis and untreated lymphomas of the abdominal lymph nodes [44, 45] (Fig. 16). Enlarged lymph nodes with a low-attenuation center can also be seen in pyogenic infection and Whipple's disease [44, 46].

Complicated Ascites

Complicated ascites (hemorrhagic or infected) will appear as a multiseptate pseudomass mimicking a lymphangioma or cystic mesothelioma (Fig. 17).

Solid Masses

While the cystic masses involving the mesentery and omentum are mainly benign (teratoma, mesenteric cyst) or malignant with low-aggressiveness (cystic mesothelioma), solid masses are overtly malignant (mesothelioma, leiomyosarcoma) or characterized by highly aggressive behavior (fibromatosis). There is a wide range of solid masses involving the mesentery and omentum [47] (Table 3).

Infectious Diseases

Tuberculosis

In the developing world, tuberculosis continues to be an endemia, while in the West it has experienced a recent

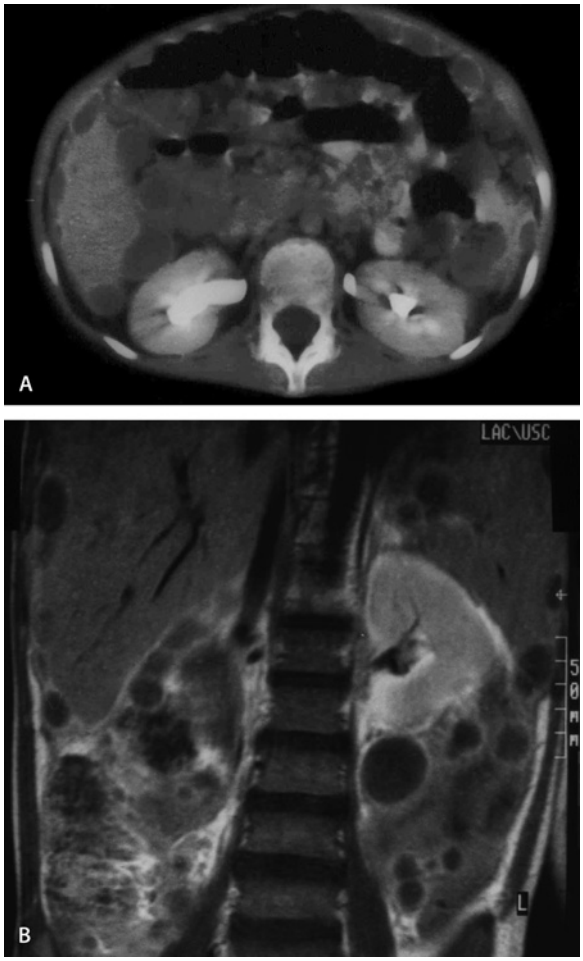

Fig. 16A, B. MAI mesenteric lymphadenopathy. **A** CT scan and **B** T1-weighted MR image of a patient with HIV and MAI infection show multiple well-circumscribed, almost cystic-appearing masses with enhancing rims

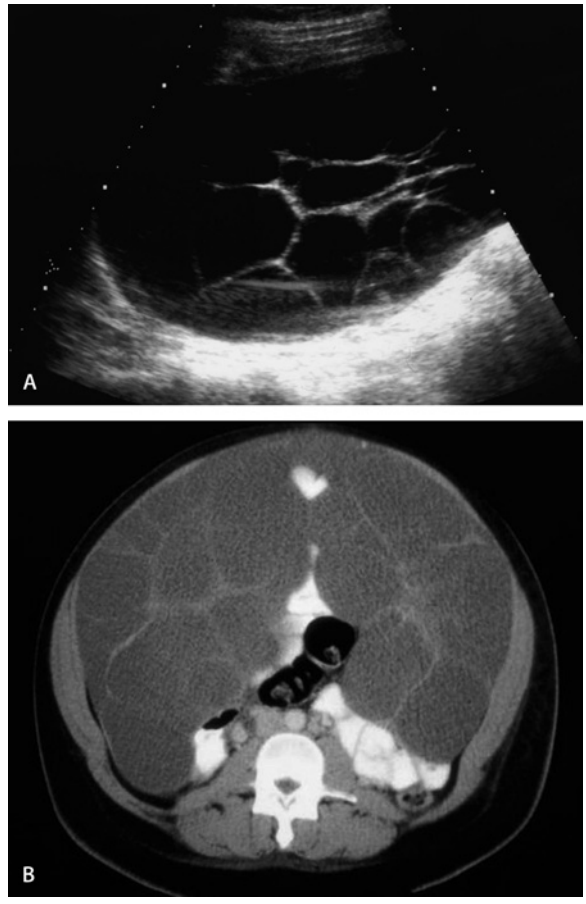

Fig. 17A, B. Infected ascites mimicking a multiseptate mass. **A** US and **B** CT scan demonstrate multi-septate cystic lesions that proved to be infected ascites

Table 3. Mesenteric/Omental Solid Masses[a]

I.	Infectious Diseases
	Tuberculosis
II.	Neoplasms
	Primary benign tumors – Lipoma – Neural tumors (neurofibroma, schwannoma, paraganglioma, ganglioneuroma)
	Primary malignant tumors – Malignant mesothelioma – Malignant fibrous histiocytoma – Spindle cell tumors (leiomyoma/leiomyosarcoma) – Liposarcoma
	Secondary tumors – Peritoneal carcinomatosis – Mesentery/omental metastases (carcinoid tumor) – Lymphoma
III.	Miscellaneous
	Fibrosing mesenteritis
	Fibromatosis or desmoid tumor
	Castleman's disease Splenosis

[a] Modified from [2] and [47]

resurgence. The increased incidence of tuberculosis has been attributed to several causes, including the AIDS epidemic, intravenous drug abuse, and increased immunocompromised patients [48].

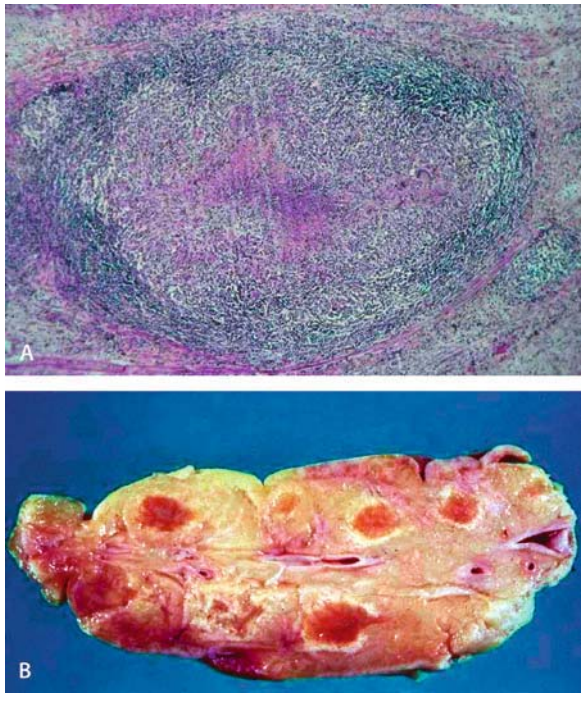

Fig. 18A, B. Tuberculosis: pathologic findings. **A** Microscopic finding of a tuberculous nodule demonstrates an inflammatory granuloma with typical caseous necrosis in the center. **B** Gross specimen shows multiple indurated nodules in the omentum

Mesenteric/omental tuberculosis occurs most frequently in immunocompromised patients. Tuberculosis within the abdomen can potentially infect all abdominal organs. Possible mechanisms in development of abdominal tuberculosis include hematogenous or lymphatic dissemination from a distant focus, usually in the lung, and ingestion of infected milk or sputum [49].

Pathologic Findings

The causative organism is usually *M. tuberculosis hominis*, or atypical mycobacteria (*M. avium-intracellulare*). As elsewhere in the body, tuberculosis in the abdomen forms granulomas with typical caseous necrosis (Fig. 18). These may present clinically as ulcers or masses (tuberculoma).

Grossly, tuberculous granulomas aggregate to confluent masses, replacing the fat in the greater omentum and forming the so-called "omental cake pattern" [50].

Imaging Features

Abdominal tuberculosis may mimic a large variety of conditions such as lymphoma, inflammatory bowel diseases, or other gastrointestinal tumors. Lymphadenopathy in mesentery or omentum is a common manifestation of abdominal tuberculosis.

CT demonstrates mesenteric and omental tuberculous masses with replacement of the normal fat by enhancing, high-attenuation masses that may contain small islands of normal fat (Fig. 19). Tuberculous adenopathy is often identified in the mesentery. Contrast enhanced CT most commonly demonstrates peripherally enhancing lymph nodes with low-density centers reflecting the usual findings of a peripheral inflammatory reaction and central caseous necrosis [40, 48, 49].

On MRI, tuberculous adenopathy shows T1 iso- or hypointensity and central T2 hyperintensity [45] (Fig. 16). Similar patterns, however, may be seen with metastases of malignant neoplasms, Whipple's disease, and lymphoma [46, 51].

Tuberculous peritonitis is the most common presentation of abdominal tuberculosis. The several patterns of tuberculous peritonitis are described: wet, fibrotic, and dry types. The wet type, characterized by large amounts of free or loculated viscus fluid, is most common. CT demonstrates the nonspecific appearance of ascitic fluid with high Hounsfield units (25–45 HU) [52] (Fig. 20). The fibrotic-fixed type is less common and characterized by omental masses, matted and tethered bowel loops and mesentery. The dry type is unusual and characterized by caseous nodules, fibrous calcified or noncalcified peritoneal reaction, and dense adhesions. Similar peritoneal features may occur with carcinomat-

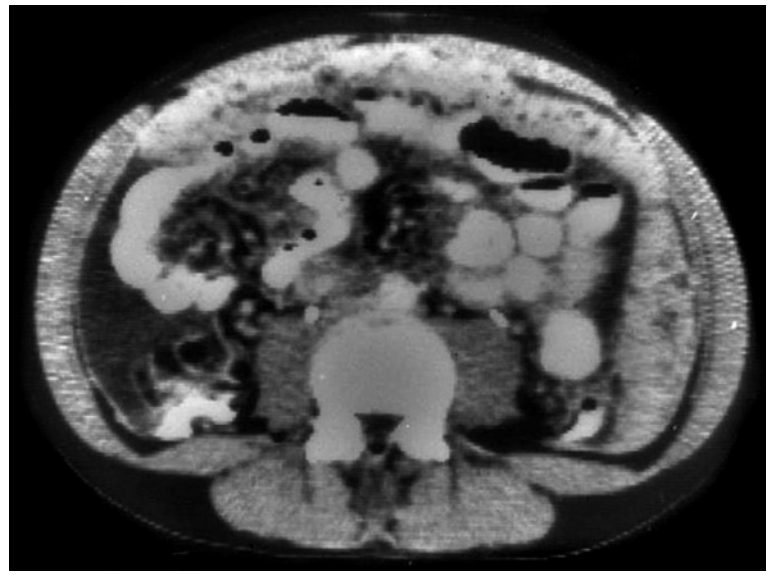

Fig. 19. Tuberculosis. Axial CT scan demonstrates mesenteric and omental high-attenuation masses that may contain small islands of normal fat

Fig. 20. Tuberculous peritonitis. Contrast-enhanced CT scan of abdomen shows nonspecific ascitic fluid with high Hounsfield units. Note the enhancement of thickened peritoneum

osis, mesothelioma, and non-tuberculous peritonitis. Although there are occasionally difficulties of a differential diagnosis, a high degree of clinical suspicion and the imaging features may allow early diagnosis of mesenteric and omental tuberculosis.

Neoplasms

Lipoma, liposarcoma

Lipoma/liposarcoma arises from adipose tissue and is the most common soft tissue tumor. While in the retroperitoneum liposarcomas are the most common neoplasms, in the mesentery lipomas are much more common. Lipoma is the second most frequent mesenteric primary tumor after fibromatosis [2].

Pathologic Findings

Histologically, liposarcomas are classified as well-differentiated, myxoid, pleomorphic, and round-cell subtypes. Prognosis for patients with liposarcoma varies on the basis of the histologic subtype [53, 54].

Imaging Features

Although the site of origin cannot be determined before surgery, the diagnosis of lipoma is made relatively easily with US, CT, or MRI. Well-differentiated liposarcomas can have two subtypes: fatty or lipoma-like and fibrous or sclerosing liposarcoma. Lipoma and lipoma-like liposarcoma demonstrate a well-defined mass, with negative attenuation values on CT images or with hyperintensity in T1-weighted MR images. It may be impossible to differentiate this type of liposarcoma from benign lipoma, although internal septations are unusual for lipoma [55]. The sclerosing type of liposarcoma demonstrates the CT attenuation or MR signal intensity that approximate the characteristics of muscle, and enhances homogeneously on contrast enhanced CT or MR images. Less differentiated liposarcomas have myxoid and pleomorphic subtypes. Myxoid components show CT attenuation and MR signal intensity similar to that of water. After contrast enhancement, gradual reticular enhancement can be seen within the myxoid components. Some areas of myxoid liposarcoma may enhance markedly. Pleomorphic components show similar attenuation than muscle on CT images and signal intensity on T1-weighted MR images (Fig. 21). On T2-weighted MR images, however, they have signal intensity equal to that of fat (Fig. 22). Thus the pleomorphic component differs from the sclerosing component in MR signal intensity.

Fig. 21. Pleomorphic liposarcoma. Axial CT scan demonstrates a large mesenteric mass with mainly solid in density

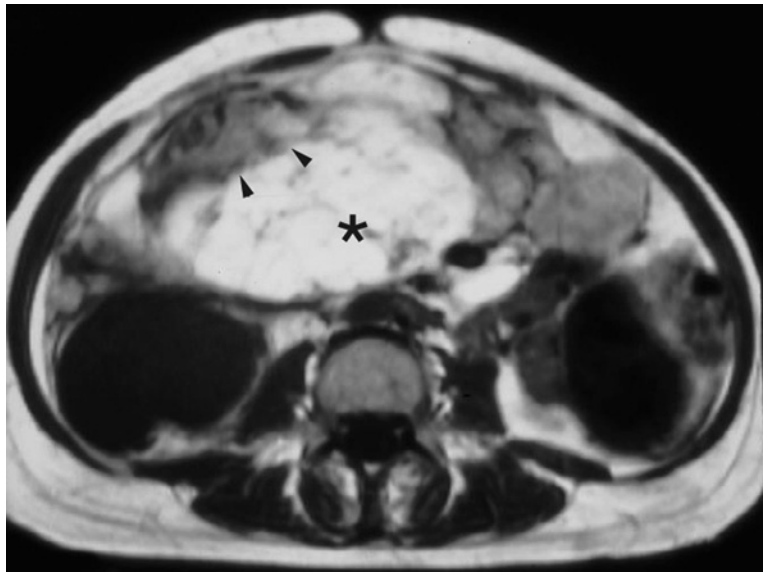

Fig. 22. Liposarcoma, MRI appearance. T1-weighted spin-echo image demonstrates a large mass in the mesentery with predominantly high signal intensity (*). There are peripheral components of lower signal intensity corresponding to areas with sarcomatous contents (*arrowheads*). Note multiple fibrous septa

The round-cell type liposarcoma demonstrates similar attenuation and signal intensity to that of muscle. It appears heterogeneous, while the sclerosing component is relatively homogeneous on contrast-enhanced CT images [54].

The combination of two or more histologic components in a tumor occurs commonly and results in the combined characteristics of the individual subtypes.

Neural Tumors (Neurofibroma, Schwannoma)

Most benign nerve sheath tumors are either schwannoma or neurofibroma [56]. Schwannoma arises from Schwann cell of the peripheral nerve sheaths. Schwannoma is a slow-growing benign tumor with favorable prognosis. It occurs without sex predominance in the 30–60-year age group [57]. They generally occur as a solitary mass located in the deep soft-tissue commonly in the head and neck, mediastinum, retroperitoneum, pelvis, presacral location or in an extremity [58]. The patient presents with a slowly expanding mass that may or may not be symptomatic, depending on its location.

Neurofibroma is a benign neoplasm consisting of fibroblasts, Schwann cells and nerve's elements that expand and diffusely infiltrate the nerve. Neurofibromas may appear sporadically, or in patients with neurofibromatosis without a sex predilection. They rarely can degenerate into a neurofibrosarcoma.

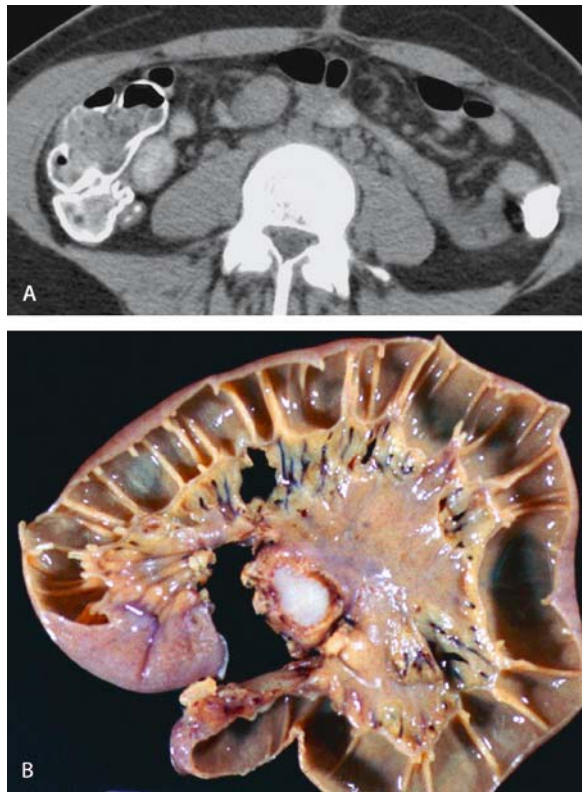

Fig. 23A, B. Schwannoma. **A** Axial CT scan demonstrates a small well-circumscribed, homogeneous soft tissue mass in the mesentery. **B** Cut section of resected specimen shows whitish mass with no necrosis

Pathologic Findings

Schwannomas are composed of Antoni type A (cellular pattern) and B (sparsely cellular pattern) areas. These lesions begin as solid tumors but as they become larger, they undergo spontaneous degeneration with areas of hemorrhage and cystic changes.

Typically in the abdomen, neurofibromas are massive and plexiform (involving multiple continuous nerves), or forming discrete masses along the same nerve. They are gelatinous in consistence and homogeneous in composition.

Imaging Features

On CT they appear as well-circumscribed masses. Although the presence of calcification on histology is common, on CT calcification is not usually evident (Fig. 23). The majority of these tumors are hypervascular, showing an intense contrast enhancement. Schwannomas are often heterogeneous and are generally isointense to muscle on T1-weighted images and hyperintense on T2-weighted images. The presence of a low-signal capsule is more suggestive of a schwannoma than of a neurofibroma [59].

On CT, neurofibromas appear of low-density because of their myxoid matrix. They displace vessels and involve the root of the mesentery without producing bowel obstruction or biliary dilatation (Fig. 24). Simple neurofibromas are usually smooth, well-demarcated, homogeneous, hypodense masses relative to muscle. They enhance homogeneously with contrast material. Low CT density less than muscle is related to the high lipid and water content in the mucinous matrix, entrapment of perineural adipose tissue, and cystic degeneration [57].

On MRI a target pattern with peripheral hyperintense rim and central low intensity has been described in 50% of peripheral nerve sheath tumors but this distinguishing feature is unlikely to be present in schwannomas due to degenerative changes [60–62]. The high T2 signal, enhanced peripheral component of the tumor represents myxomatous tissue, whereas the central low T2 signal, hypovascular area represents fibrous and collagenous material [62] (Fig. 25). This zonal pattern does not correlate histologically with the proportion of Antoni-A and Antoni-B type tissue present [63].

Fig. 24. Neurofibroma. Contrast enhanced CT scan demonstrates low attenuation mass involving mesenteric root and porta hepatis

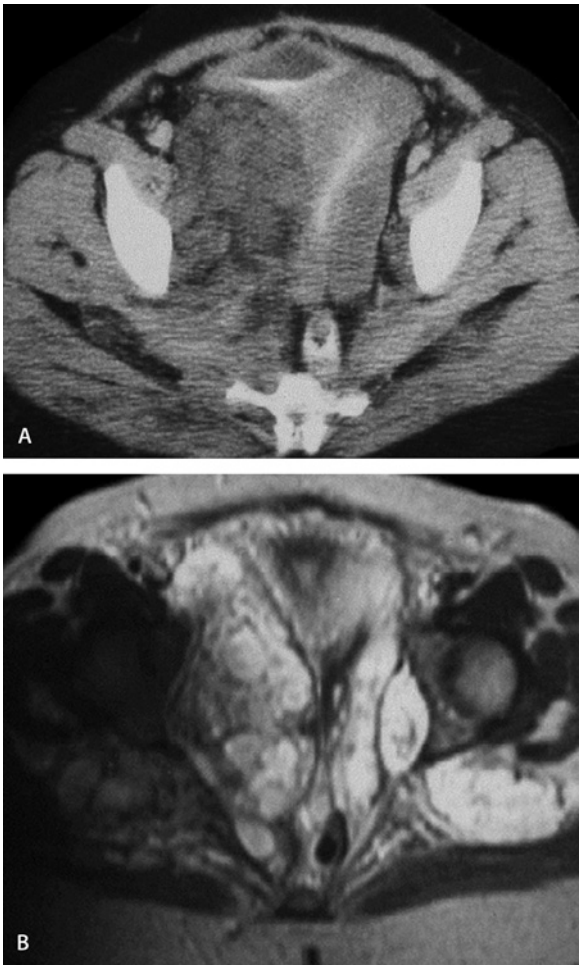

Fig. 25A, B. Neurofibroma, MRI appearance. **A** Axial CT shows low attenuation soft tissue mass in right pelvic cavity. **B** T2-weighted MR image demonstrates the high signal intensity of the lesion due to myxoid component

Malignant Mesothelioma

Malignant mesothelioma is the primary malignancy of the peritoneum. While the majority originate in the pleura, 25% of cases arise in the peritoneum. The association of asbestos exposure is higher with peritoneal than with pleural mesothelioma. The prognosis is extremely poor. It presents usually in men with a history of prior asbestos exposure.

Pathologic Findings and Imaging Features

Three different types of peritoneal malignant mesothelioma are recognized histologically with different growth patterns and radiological appearance: (1) carcinomatous, (2) sarcomatous, and (3) biphasic or mixed. The carcinomatous type appears as diffuse thickening of the peritoneum with small nodular plaques in the mesentery, producing crowning, fixation and diffuse thickening of the small bowel (Fig. 26). Both parietal and visceral peritoneum are involved. Sarcomatous, peritoneal mesothelioma presents as a large encapsulated mass, similar in appearance to spindle cell tumors (leiomyoma/leiomyosarcoma) (Fig. 27). The biphasic or mixed type presents as both a band of tissue involving the peritoneal surfaces and masses. Regardless of the histological subtype, pleural plaques and calcification due to asbestos exposure can be present in approximately 70% of cases [64] (Fig. 27). Gadolinium enhanced breath hold fat-saturated MRI may reveal more peritoneal tumors than CT, especially when ascites is present.

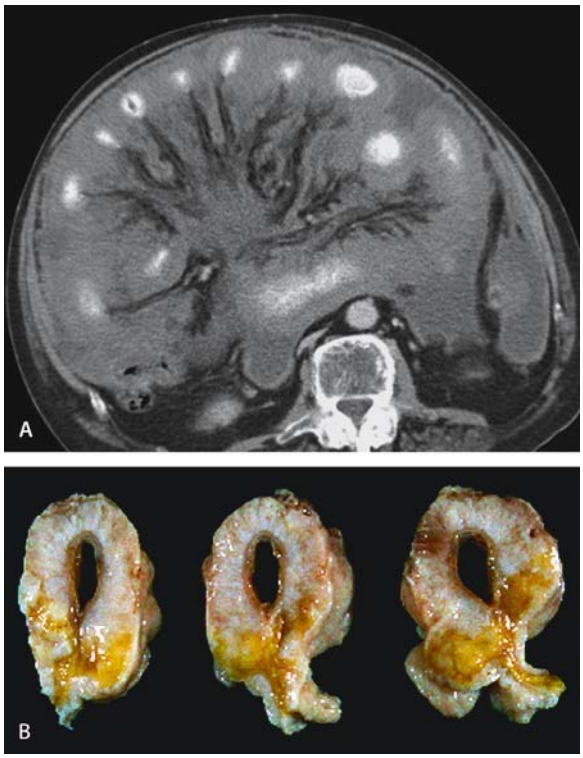

Fig. 26A, B. Malignant mesothelioma (carcinomatous form). **A** CT scan demonstrates thickening of both parietal and visceral peritoneum. Note how mesothelioma surrounds multiple loops of bowel and extends into the mesentery. **B** Cut sections of the specimen show the diffuse tumor infiltration and bowel wall thickening

Malignant Fibrous Histiocytoma

Malignant fibrous histiocytoma (MFH) is one of the most common sarcomas appearing in late adult life. Typically it appears in the fifth and sixth decades of life. It frequently occurs in the soft tissue of the extremities, the retroperitoneum and in the bone [65–69]. Despite this ubiquity, involvement of the peritoneal cavity is uncommon.

Pathologic Findings

MFH is typically manifested as a broad range of histopathological appearances and is currently classified into four subtypes: storiform-pleomorphic, myxoid, giant cell, and inflammatory. Microscopically MFH consists of areas of spindle cells arranged in a storiform pattern, and pleomorphic areas with haphazardly arranged sheets of fibroblasts and histiocytes [66, 67]. Calcification is common [68–71].

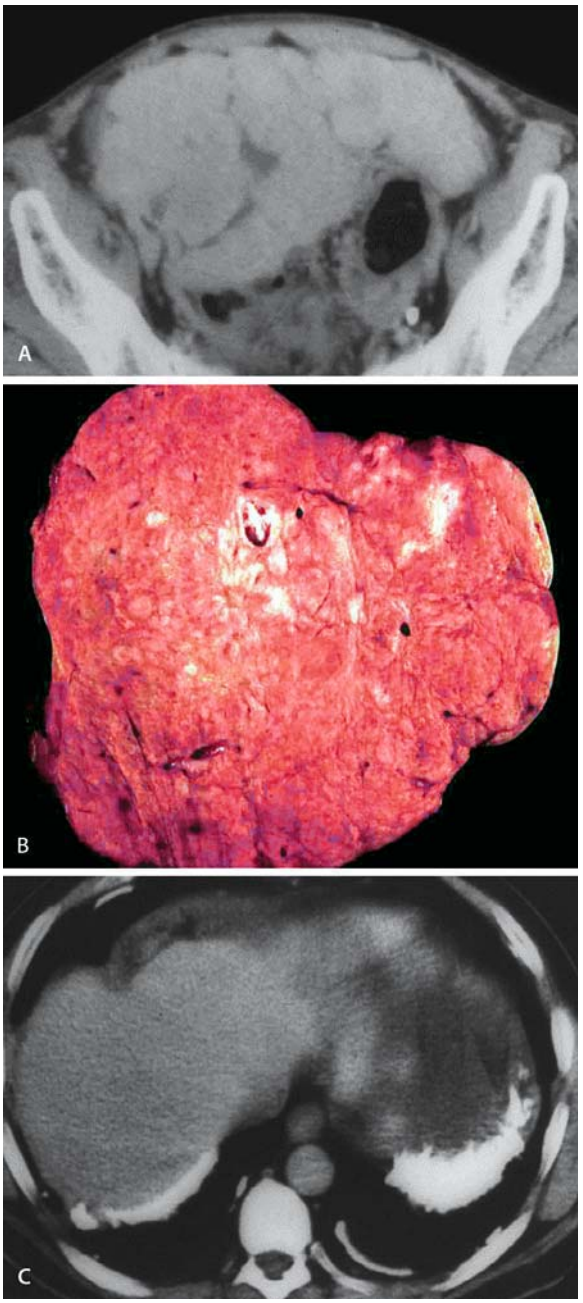

Fig. 27A–C. Malignant mesothelioma (sarcomatoid form). **A** Axial CT scan and **B** resected specimen demonstrate large mass with similar imaging features to stromal cell tumor. **C** CT shows pleural calcification plaque suggestive of asbestos exposure

Imaging Features

Imaging features of MFH are nonspecific and most examples of MFH appear as heterogeneous solid masses with areas of necrosis [68–71]. A variety of patterns have been reported on ultrasound, including hypoechoic, mixed (due to tumor necrosis) or predominantly an-

echoic with thick septa. MFH generally presents as a hypoechoic or heteroechoic solid mass [69, 70].

On CT, MFH typically presents as a poorly marginated or well-circumscribed mass, with a density similar to or slightly less than that of normal muscle and with hypodense areas due to necrosis [68–71]. Eccentrically located lumpy and ring-like calcifications due to osteoid and chondroid metaplasia have been reported on CT in 16% of abdominal MFH [71]. Tumor invasion of contiguous organs are common [68]. Occasionally MFH with extensive necrosis may be manifested as a cystic tumor [72, 73]. Extensive intratumoral hemorrhage may occur, creating a cyst-like tumor that may be confused with hematoma [67, 74].

MRI demonstrates the tumor usually of intermediate to low signal intensity on T1-weighted images. With T2-weighted images, the tumors tend to be of high signal intensity, although often quite inhomogeneous centrally [75].

Spindle Cell Tumor (Leiomyoma/Leiomyosarcoma)

Spindle cell tumor or smooth muscle tumor are preferred terms for mesenteric/omental leiomyoma/leiomyosarcoma. Leiomyosarcoma is more common in the mesentery than leiomyoma [76].

Pathologic Findings

Grossly, spindle cell tumors usually have central areas of necrosis, adenoma and hemorrhage (Fig. 28). Leiomyosarcomas are usually large, with invasion of surrounding structures. They often contain no fat or calcification [77, 78].

Imaging Features

By US and CT, leiomyosarcomas usually appear as large and heterogeneous masses. They are predominantly

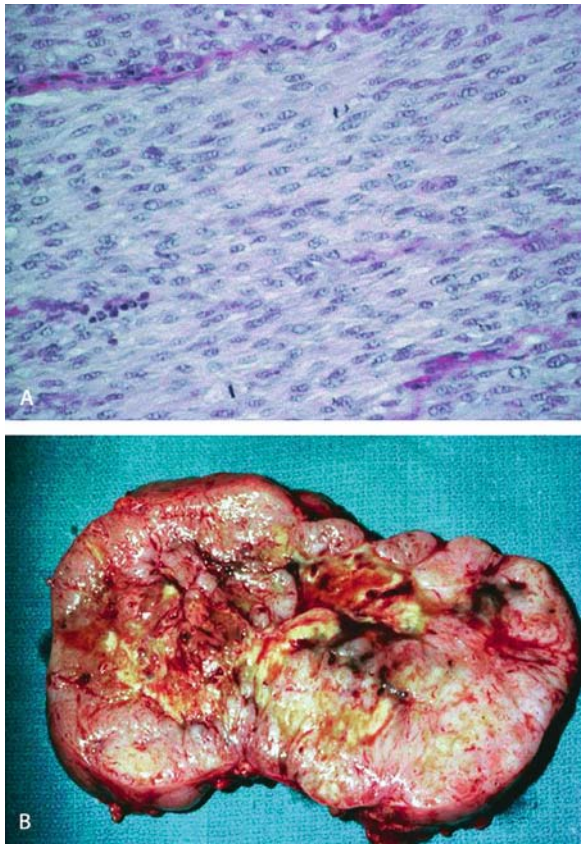

Fig. 28A, B. Spindle cell tumor (leiomyosarcoma): pathology. **A** Photomicrograph demonstrates tumors with spindle cells in bundles. **B** Gross specimen shows a large solid mass lesion with multiple cystic spaces suggesting central necrosis

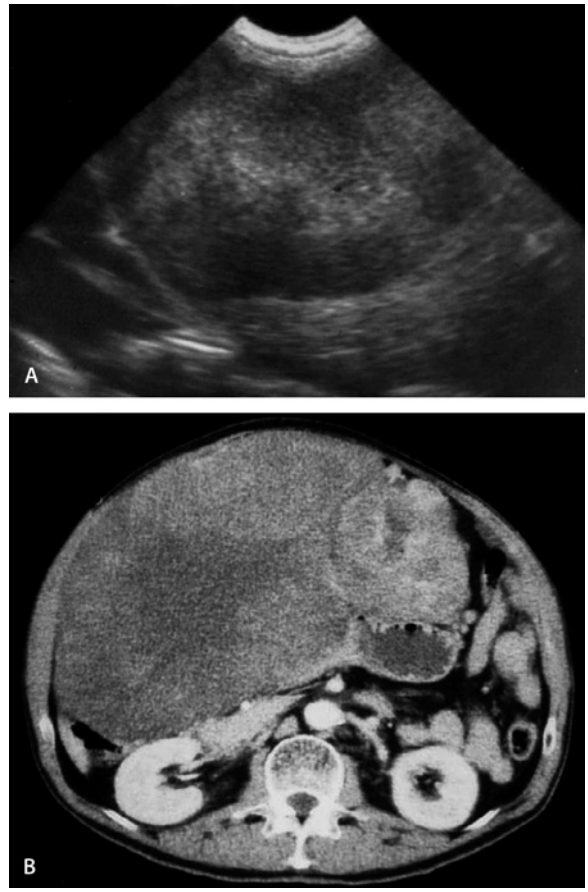

Fig. 29A, B. Spindle cell tumor (leiomyosarcoma). **A** Ultrasonogram and **B** contrast enhanced CT scan demonstrate a huge solid mass with heterogeneous center

solid with internal cystic spaces, correlating with areas of necrosis grossly [79] (Fig. 29).

On MRI the mass is usually heterogeneous with low to intermediate signal intensity on T1-weighted images and with intermediate to high signal intensity on T2-weighted images. Intratumoral necrosis is evident as a high intensity central zone on T2-weighed images, without enhancement [77, 78].

Lymphoma, Metastasis

Peritoneal carcinomatosis, carcinoid metastases and lymphoma are three common secondary malignancies that may involve the mesentery and omentum.

Primary mesenteric lymphoma, usually non-Hodgkin lymphoma, is a disease of the mesenteric lymph nodes that may appear as a localized process or a component of a more disseminated pattern of disease. A few cases of mesenteric lymphomas observed in association with AIDS, immune thrombocytopenia, and dermatitis herpetiformis have been reported [80]. The clinical presentation of mesenteric lymphoma is much like that of other mesenteric tumors, with abdominal pain and a palpable mass as the principal findings.

The vast majority of metastatic lesions of the mesentery consist of mesenteric lymph nodes that have become secondarily involved in a neoplastic process of the tubular gastrointestinal tract. Distinguishing this pattern of tumor growth from primary mesenteric tumors usually presents no difficulty because the gastrointestinal primary tumor is usually readily identifiable.

Pathologic Findings

The appearance is variable, with lymphoma and carcinomatosis frequently appearing as multiple masses with variable degrees of involvement and carcinoid metastases seen typically as a mesenteric mass producing kinking and retraction of adjacent bowel loops and with frequent calcification [81]. This is due to the notable desmoplastic reaction seen with carcinoid tumors.

Imaging Features

CT is the preferred imaging modality for evaluation of the mesentery in patients presenting with lymphoma. With lymphoma, bulky paraaortic lymphadenopathy is common (Fig. 30). Enlarged lymph nodes may appear as discrete masses or as confluent soft tissue obliterating the mesenteric fat, resulting in loss of definition of fat planes between the other organs. Many other lymph node groups, such as retrocrural, gastrohepatic, paraceliac, periportal, peripancreatic, posterior iliac crest, and pelvic chains are frequently involved [82]. CT scans can characterize the lesion from the standpoint of size and mesenteric location and can raise the probability of the lymphoma diagnosis [83].

Carcinoid metastases are seen typically as mesenteric masses producing kinking and retraction of adjacent bowel loops and with frequent calcification [81]. This is due to the notable desmoplastic reaction seen with carcinoid tumors (Fig. 31).

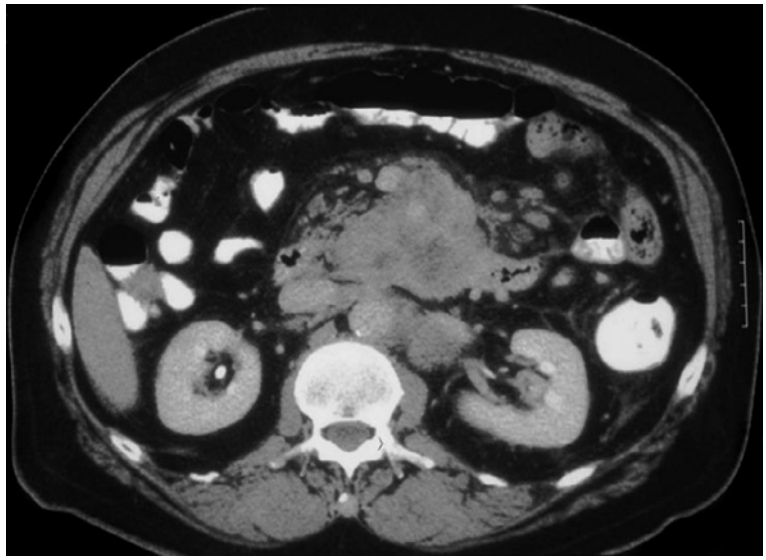

Fig. 30. Lymphoma. Axial CT scan demonstrates an irregular marginated soft tissue nodule in mesentery. Note the para-aortic lymphadenopathy

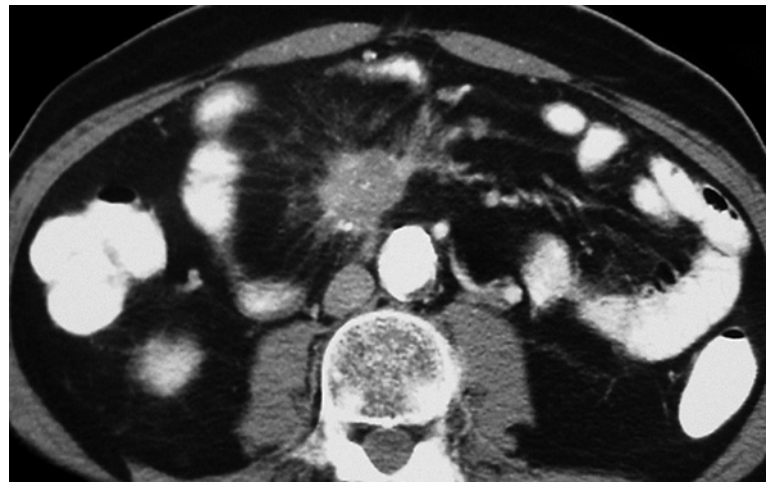

Fig. 31. Carcinoid tumors involving mesentery. Axial CT scan demonstrates a soft tissue mass with peripheral radiating strands in mesentery. Note the calcification in the mass and mural thickening of adjacent small bowel

MRI is able to demonstrate similar findings in carcinoid tumors, including the primary tumor, mesenteric metastases, and liver metastases. Liver metastases are commonly hypervascular on postgadolinium images [84].

Miscellaneous Solid Mesenteric/Omental Lesions

Fibrosing Mesenteritis (Mesenteric Panniculitis)

Fibrosing mesenteritis is a rare condition that can be mistaken for a mesenteric neoplasm based on clinical, radiologic, and gross characteristics. Fibrosing mesenteritis is part of the same process that includes other terms such as mesenteric lipodystrophy, sclerosing (retractile) mesenteritis, and mesenteric panniculitis. They

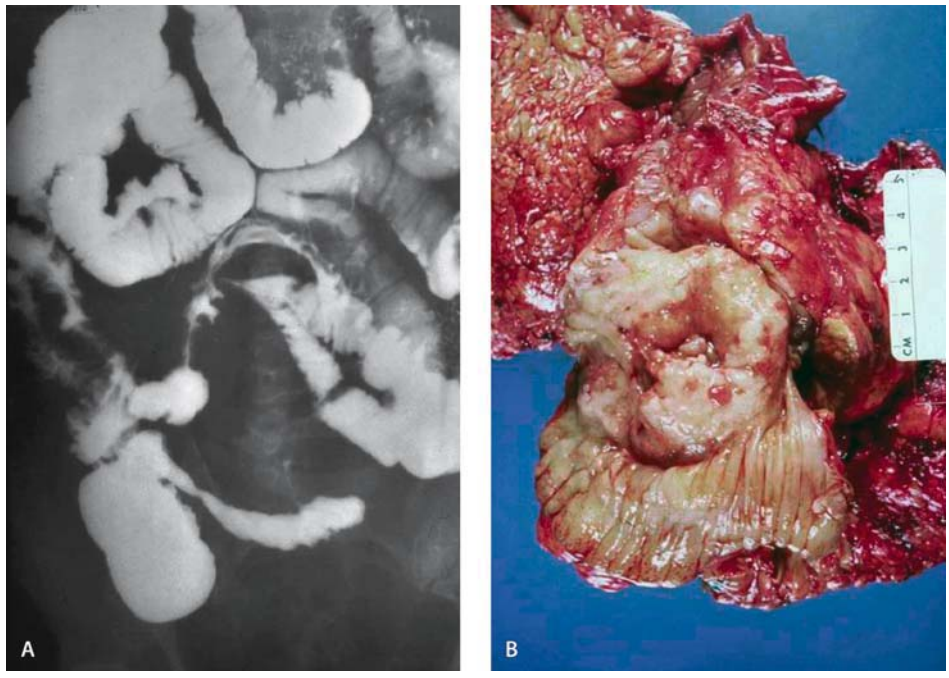

Fig. 32A, B. Sclerosing mesenteritis. **A** Barium follow-thorough demonstrates kinking and displacement of ileum due to the mass. **B** Gross specimen shows mesenteric mass formation with encasing small bowel segments

are all infiltrative mesenteric processes, with fatty, inflammatory and fibrosing components. The causative agents are unknown, although an association with lymphoma has been reported. The likely cause for fibrosing mesenteritis is trauma or other injury to the mesentery [85, 86]. Fibrosing mesenteritis has a self-limited course, with resection only necessary when there is mechanical bowel obstruction.

Its presenting symptom is abdominal pain in most patients, although it has been anecdotally reported in association with fever, mesenteric calcifications, and protein-losing enteropathy.

Pathologic Findings

Grossly, fibrosing mesenteritis shows a firm, rubbery, fibrous mass that can be either focal or diffuse within the small intestinal mesentery. The root of the mesentery and the tissues surrounding the superior mesenteric vessels are invariably involved (Fig. 32).

Histologically it consists of hypertrophied fatty tissue, dense fibrous tissue, fat necrosis, or combinations of these, along with a nonspecific chronic inflammatory infiltrate with possible calcification.

Imaging Features

Barium study may demonstrate kinking or displacement of bowel loops due to mesenteric fibrous mass formation within the intestinal mesentery (Fig. 32).

By CT, fibrosing mesenteritis may appear as a soft tissue density or heterogeneous mass, with possible calcifications [87, 88] (Fig. 33). Puckering of adjacent small bowel loops are seen. In MRI, fibrosing mesenteritis appears as a low signal intensity mass in all sequences, suggesting mature fibrotic tissue [89–91].

Fibromatosis (Desmoid Tumor)

Fibromatosis (desmoid tumor) is a non-neoplastic locally aggressive growth of fibroblastic tissue. Mesenteric fibromatosis (MF) is considered the most common primary solid mass of the mesentery. These tumors are areas of progressive fibroblastic and fibrous proliferation within the mesentery (and less frequently, the retroperitoneum or omentum) that can locally involve vascular structures and can constrict and obstruct the bowel. Although described as histologically benign lesions, their infiltrative pattern of growth can ultimately lead to life-threatening patterns of visceral involvement [92].

Although MF occurs sporadically, it may be associated with familial adenomatous polyposis (FAP). MF is identified in 20 percent of asymptomatic FAP patients [93]. MF was originally reported as a component of Gardner syndrome, a phenotypic pattern of FAP that, in addition to intestinal adenomatous polyps, is also associated with bony abnormalities, pigmented ocular fundus lesions, and cutaneous epidermoid cysts and fibromas. Prior surgery and local trauma are also frequently noted preceding the formation of mesenteric fibromatosis [94]. Although a causative relationship in fibromatosis formation has not been firmly established, various mutations of the *APC* gene have been identified in these tumors [95].

Fig. 33. Sclerosing mesenteritis, CT appearance. Enhanced CT of the abdomen demonstrates a mass in the mesentery with multiple calcifications. Note also the retraction and puckering of multiple loops of small and large bowel

Pathologic Findings

Fibromatosis is usually a large mass with no capsule. It may have whitish scar tissue within it. It rarely has areas of necrosis or hemorrhage because it is a mass with benign histologic features. Histologic specimen shows orderly arrangement of fibroblasts with uniform spine-shaped nuclei admixed to a variable amount of collagen and mucoid matrix [93] (Fig. 34).

Imaging Features

Ultrasonography demonstrates homogeneous hypoechoic mass with no signs compatible with cystic degeneration or areas of diminished echogenicity suggestive of necrosis [96] (Fig. 35). By CT imaging, a mass with sharply defined margins is seen with homogeneous density that has variable attenuation or en-

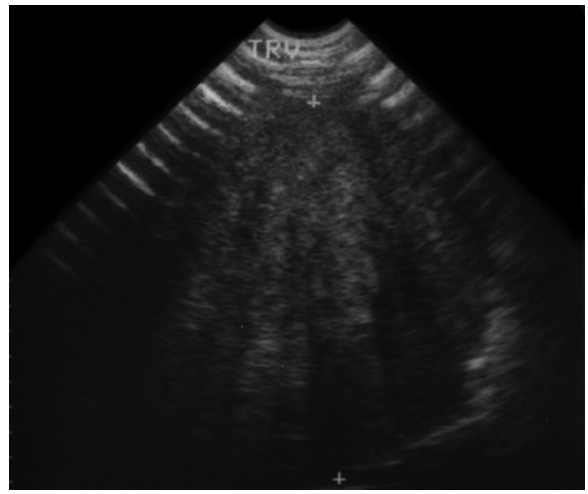

Fig. 35. Fibromatosis, US finding. Ultrasonogram demonstrates a homogeneous soft tissue mass with no areas of diminished echogenicity suggestive of necrosis

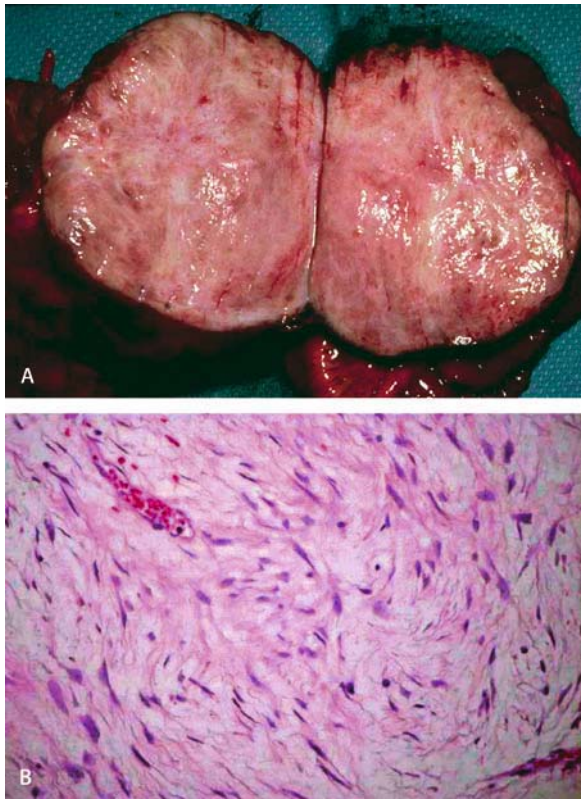

Fig. 34A, B. Pathologic findings of fibromatosis. **A** Gross specimen of fibromatosis shows a solitary fibrotic mass with no internal necrosis or hemorrhage. **B** The lesion reveals benign collagenous myxoid histologic components of typical fibromatosis

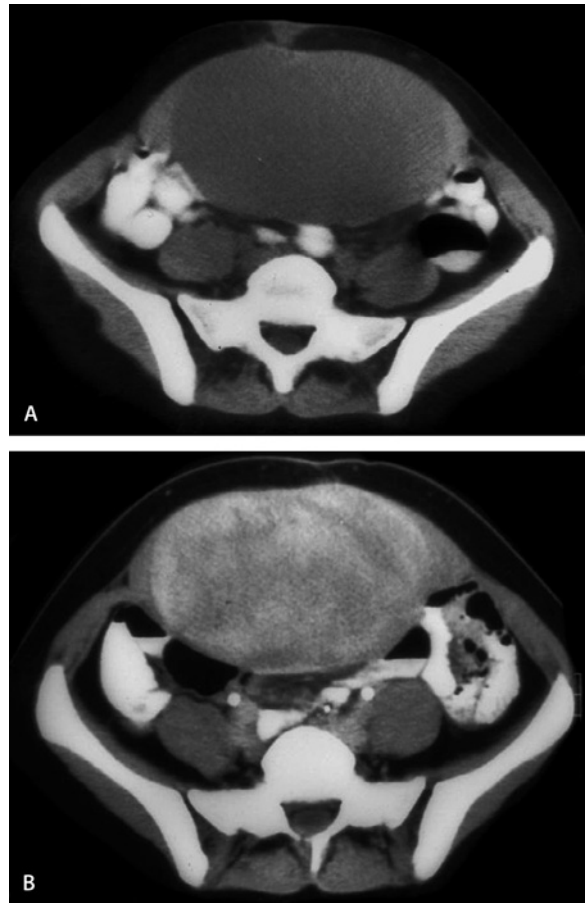

Fig. 36A, B. Fibromatosis, CT appearance. **A** Enhanced CT of the abdomen demonstrates a very large homogeneous mass. **B** After administration of contrast, there is marked enhancement of the mass, correlating with its hypervascular nature. The lack of areas of hemorrhage or necrosis is typical of mesenteric fibromatosis

hancement after contrast administration [97] (Fig. 36). MRI demonstrates fibromatosis as a mass with low signal intensity relative to muscle on T1-weighted images and variable signal intensity on T2-weighted images [98]. High signal intensity on T2-weighted images may be seen from rapidly growing fibromatosis [99] (Fig. 37).

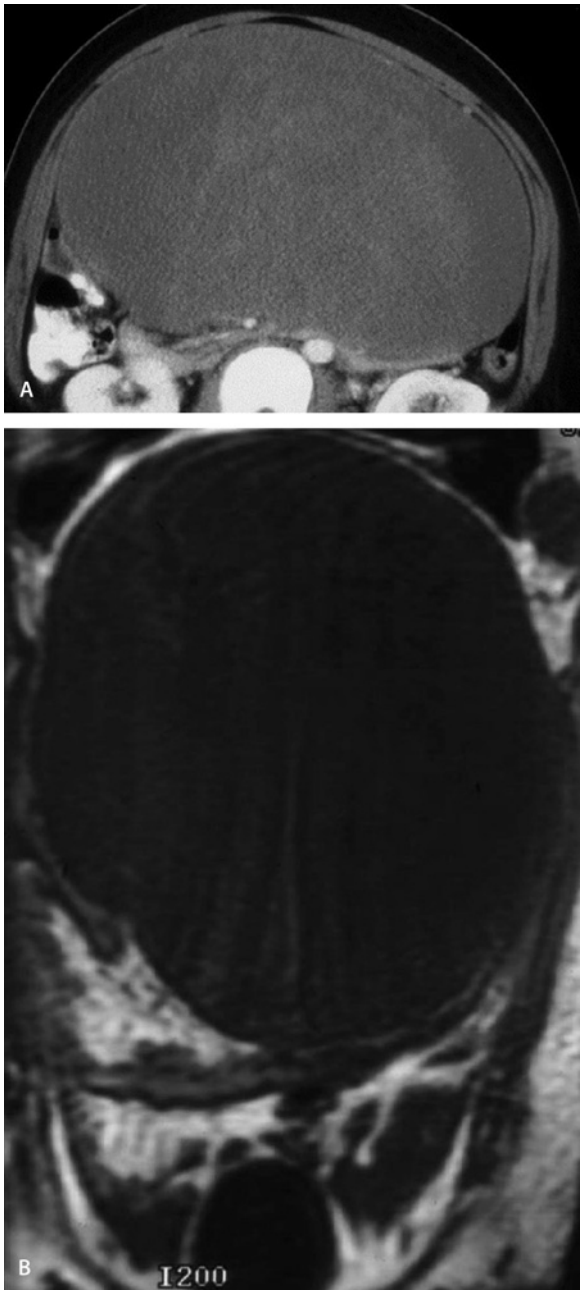

Fig. 37A, B. Fibromatosis, MRI appearance. **A** Axial CT image demonstrates a homogeneously low attenuation mass in the mesentery. **B** Coronal T1-weighted spin-echo image demonstrates a large mass in the mesentery with muscle intensity and lack of areas of necrosis or hemorrhage

Castleman's Disease

Castleman's disease is an uncommon benign lymphoproliferative disorder characterized by hyperplasia of lymphoid follicles [100]. Castleman's disease may occur anywhere along the lymphatic chain, but the mediastinum is the most common location (70%). Extrathoracic sites have been reported in the neck, axilla, pelvis, pancreas, adrenal, mesentery, and retroperitoneum [101]. Clinically, patients are usually asymptomatic, although sometimes associated with systemic manifestations such as fever, anemia, weight loss, night sweat, and polyclonal hypergammaglobulinemia [102]. Castleman's disease with systemic symptoms is usually bad in prognosis.

Pathologic Findings

There are two major histologic variants: The hyaline-vascular type, which is more frequent, is characterized by small hyaline-vascular follicles and interfollicular capillary proliferation; the plasma cell type is characterized by large follicles with intervening sheets of plasma cells [101].

Calcification and central stellate fibrosis is not uncommon in hyaline-vascular Castleman disease [102].

Imaging Features

The characteristic feature of localized Castleman disease at CT is a well-defined, homogeneous, single mass of soft tissue attenuation with or without satellite nodules (Fig. 38). The degree of enhancement may vary from mild to strong according to the histologic type [103]. Typically dynamic CT reveals the early strong enhancement and delayed washout in hyaline-vascular type [104]. Plasma cell type does not show strong enhancement. Small lumpy calcifications may be seen in the center of the mass.

The central fibrosis in hyaline-vascular type may be demonstrated as interspersed area of low attenuation on CT and hypointense on both T1- and T2-weighted MR images [105].

No radiologic finding is pathognomonic for disseminated Castleman's disease [101, 106].

Splenosis

Splenosis is the autotransplantation of residual fragments of splenic tissue in the abdomen and occasionally in the pelvis or thorax, following splenectomy typically performed for traumatic splenic injury. The most commonly involved site is the peritoneal cavity. These

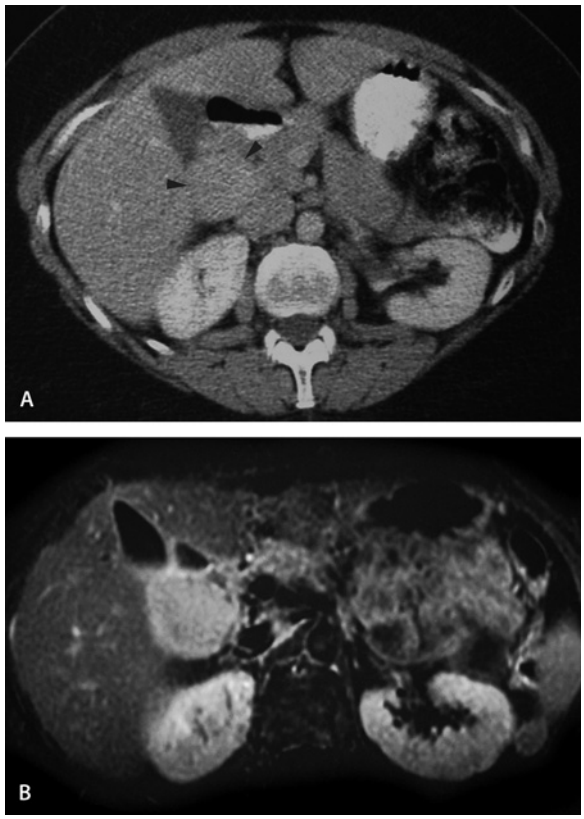

Fig. 38A, B. Castleman disease. **A** Axial CT scan demonstrates a soft tissue mass (*arrowheads*) in peripancreatic portion. **B** Gadolinium-enhanced axial T1-weighted image illustrates a large mass displacing the IVC posteriorly. The mass shows intense enhancement (nearly equal to kidneys)

foci of splenic tissue subsequently grow and regenerate nodules of functional splenic tissue [107]. Splenosis rarely becomes symptomatic in cases with infarction or spontaneous hemorrhage of intraperitoneal nodule, gastrointestinal wall implant, or recurrence of hematologic diseases (congenital hemolytic anemia, idiopathic thrombocytopenic purpura, etc) [108].

Pathologic Findings

Peritoneal splenosis may exhibit multiple round or oval peritoneal nodules. Nodules of splenosis do not exhibit a well-defined hilus. Most are up to 3 cm across but nodules up to 7 cm in greatest dimension have been reported [107].

Histological finding of splenosis may vary, but it may exhibit read and white pulp that appears histologically and immunohistochemically indistinguishable from normal or accessory spleen [109].

Imaging Features

The characteristic feature of splenosis at ultrasound, CT, and MRI is multiple well-defined, round or oval, homogeneous masses of soft tissue attenuation [110]. They enhance uniformly with intravenous contrast medium.

MRI usually demonstrates hypointense signal of the nodules on both T1- and T2-weighted MR images, identical to those of the normal spleen [111].

If necessary, their splenic origin can be confirmed with Tc-99m-tagged, heat-damaged red blood cells or sulfur colloid scintigraphy [112].

Conclusion

A wide range of entities may involve the mesentery and omentum. The radiologist must be aware of the pathological changes commonly encountered, not only for ensuring improvement in interpretation of imaging features but also for formulating a reasonable differential diagnosis.

CT, US, or MR imaging allows detecting the origin of an abdominal mass as mesenteric/omental and whether it is solid or cystic in nature. If the mass is cystic, the differential diagnosis should include benign mesenteric/omental cysts, such as cystic teratoma, cystic mesothelioma, and pseudocyst. However, it is important to remember that some malignant neoplasms, such as spindle cell tumors, can occasionally have massive cystic change and appear cystic by imaging.

Although there is substantial overlap in imaging features, it should be remembered that most solid masses involving the mesentery/omentum are neoplastic and most are secondary malignant tumors. It is also important to consider the possibility of tuberculosis or lymphoma, since these entities are usually treated with medical therapy, and surgery should be avoided.

■ **Acknowledgements.** The authors are grateful to Seth Levine for editorial assistance in preparing the manuscript.

References

1. Stoupis C, Ros PR, Abbitt PL, Burton SS, Gauger J (1994) Bubbles of the belly: imaging of cystic mesenteric or omental masses. RadioGraphics 14:729–737
2. Hamrick-Turner JE, Chiechi MV, Abbitt PL, Ros PR (1992) Neoplastic and inflammatory processes of the peritoneum, omentum, and mesentery: diagnosis with CT. RadioGraphics 12:1051–1068
3. Kurtz R, Heimann T, Holt J (1986) Mesenteric and retroperitoneal cysts. Ann Surg 203:109–112
4. Takiff H, Calabria R, Yin L (1985) Mesenteric cysts and intra-abdominal cystic lymphangiomas. Arch Surg 120:1266–1269

5. Vanek V, Phillips A (1984) Retroperitoneal, mesenteric, and omental cysts. Arch Surg 119:838–842
6. Egozi E, Ricketts R (1997) Mesenteric and omental cysts in children. Am Surg 63:287–290
7. Bliss DJ, Coffin C, Bower R (1994) Mesenteric cysts in children. Surgery 115:571–577
8. Walker A, Putnam T (1973) Omental, mesenteric, and retroperitoneal cysts: a clinical study of 33 new cases. Ann Surg 178:13–19
9. Singh S, Baboo ML, Pathak IC (1971) Cystic lymphangioma in children: report of 32 cases including lesions atrrare sites. Surgery 69:947–951
10. Ros PR, Olmsted WW, Moser RP Jr, Dachman AH, Hjermstad BH, Sobin LH (1987) Mesenteric and omental cysts: histologic classification with imaging correlation. Radiology 164: 327–332
11. Ko SF, Ng SH, Shieh CS, Lin JW, Huang CC, Lee TY.1995) Mesenteric cystic lymphangioma with myxoid degeneration: unusual CT and MR manifestations. Pediatr Radiol 25:525–527
12. Davidson AJ, Hartman DS (1990) Lymphangioma of the retroperitoneum: CT and sonographic characteristic. Radiology 175:507–510
13. Lugo-Olivieri CH, Taylor GA (1993) CT differentiation of large abdominal lymphangioma from ascites. Pediatr Radiol 23:129–130
14. Stoupis C, Ros PR, Williams JL (1993) Hemorrhagic lymphangioma mimicking hemoperitoneum: MR imaging diagnosis. J Magn Reson Imaging 3:541–542
15. Forshall I (1961) Duplication of the intestinal tract. Postgrad Med J 37:570–589
16. Anderson MC, Silberman WW, Shields TW (1962) Duplications of the alimentary tract in the adult. Arch Surg 85: 94–108
17. Otter MI, Marks CG, Cook MG (1996) An unusual presentation of intestinal duplication with a literature review. Dig Dis Sci 41:627–629
18. Royle SG, Doig CM (1988) Perforation of the jejunum secondary to a duplication cyst lined with ectopic gastric mucosa. J Pediatr Surg 23:1025–1026
19. Lecouffe P, Spyckerelle C, Venel H, Meuriot S, Marchandise X (1992) Use of pertechnetate 99mTc for abdominal scanning in localising an ileal duplication cyst: case report and review of the literature. Eur J Nucl Med 19:65–67
20. Tong SC, Pitman M, Anupindi SA (2002) Best cases from the AFIP. Ileocecal enteric duplication cyst: radiologic-pathologic correlation. Radiographics 22:1217–1222
21. de Perrot M, Brundler M, Totsch M, Mentha G, Morel P (2000) Mesenteric cysts. Toward less confusion? Dig Surg 17: 323–328
22. Gourtsoyiannis NC, Bays D, Malamas M, Mouchtouris A (1993) Mesothelial cyst complicated by torsion: preoperative imaging evaluation. Hepatogastroenterology 40:509–512
23. Sardi A, Parikh KJ, Singer JA, Minken SL (1987) Mesenteric cysts. Am Surg 53:58–60
24. Bowen B, Ros PR, McCarthy MJ, Olmsted WW, Hjermstad BM (1987) Gastrointestinal teratomas: CT and US appearance with pathologic correlation. Radiology 162:431–433
25. Whang SH, Lee KS, Kim PN, Bae WK, Lee BH (1990) Omental teratoma in an adult: a case report. Gastrointest Radiol 15: 301–302
26. Ralls PW, Hartman B, White W, Radin DR, Halls J (1987) Computed tomography of benign cystic teratoma of the omentum. J Comput Assist Tomogr 11:548–549
27. Moon W, Kim Y, Rhim H, Koh B, Cho O (1997) Coexistent cystic teratoma of the omentum and ovary: report of two cases. Abdom Imaging 22:516–518
28. O'Neil JD, Ros PR, Storm BL, Buck JL, Wilkinson EJ (1989) Cystic mesothelioma of the peritoneum. Radiology 170: 333–337
29. Weiss SW, Tavassoli FA (1988) Multicystic mesothelioma. An analysis of pathologic findings and biologic behavior in 37 cases. Am J Surg Pathol 12:737–746
30. Hasan AK, Sinclair DJ (1993) Case report: calcification in benign cystic peritoneal mesothelioma. Clin Radiol 48:66–67
31. Ozgen A, Akata D, Akhan O, Tez M, Gedikoglu G, Ozmen MN (1998) Giant benign cystic peritoneal mesothelioma: US, CT, and MRI findings. Abdom Imaging 23:502–504
32. Bui-Mansfield LT, Kim-Ahn G, O'Bryant LK (2002) Multicystic mesothelioma of the peritoneum. AJR Am J Roentgenol 178:402
33. Volk BA, Scholmerich J, Farthmann E, Gerok W, Wenz W (1983) Leiomyoblastoma of the stomach–a case report on ultrasonographic differential diagnosis of cystic lesions in the abdomen. Hepatogastroenterology 30:33–35
34. McFadden DW, Hiyama D, Moulton JS, Biddinger P (1993) Primary mesenteric leiomyosarcoma masquerading as a pancreatic pseudocyst. Pancreas 8:647–9
35. Miettinen M, Monihan JM, Sarlomo-Rikala M, Kovatich AJ, Carr NJ, Emory TS, Sobin LH (1999) Gastrointestinal stromal tumors/smooth muscle tumors (GISTs) primary in the omentum and mesentery: clinicopathologic and immunohistochemical study of 26 cases. Am J Surg Pathol 23:1109–1118
36. Lee JT, Kim MJ, Yoo KS, Suh JH, Leong HJ (1991) Primary leiomyosarcoma of the greater omentum: CT findings. J Comput Assist Tomogr 15:92–94
37. Jivan S, Bahal V (2002) Pseudomyxoma peritonei. Postgrad Med J 78:170–172
38. Sulkin TV, O'Neill H, Amin AI, Moran B (2002) CT in pseudomyxoma peritonei: a review of 17 cases. Clin Radiol 57: 608–613
39. Lersch C, Frimberger E, Ott R, Classen M (2001) Gray-scale sonographic findings in a patient with pseudomyxoma peritonei. J Clin Ultrasound 29:186–191
40. Pestieau SR, Wolk R, Sugarbaker PH (2000) Congenital pleuroperitoneal communication in a patient with pseudomyxoma peritonei. J Surg Oncol 73:174–178
41. Gollub MJ, DeCorato D, Schwartz LH (2000) MR enteroclysis: evaluation of small-bowel obstruction in a patient with pseudomyxoma peritonei. AJR Am J Roentgenol 174:688–690
42. Pantongrag-Brown L, Krebs TL, Daly BD, Wong-You-Cheong JJ, Beiser C, Krause B, Brown AE (1998) Frequency of abdominal CT findings in AIDS patients with M. avium complex bacteraemia. Clin Radiol 53:816–819
43. Klatt EC, Jensen DF, Meyer PR (1987) Pathology of Mycobacterium avium-intracellulare infection in acquired immunodeficiency syndrome. Hum Pathol 18:709–714
44. Yang ZG, Min PQ, Sone S, He ZY, Liao ZY, Zhou XP, Yang GQ, Silverman PM (1999) Tuberculosis versus lymphomas in the abdominal lymph nodes: evaluation with contrast-enhanced CT. AJR Am J Roentgenol 172:619–623
45. Kim SY, Kim MJ, Chung JJ, Lee JT, Yoo HS (2000) Abdominal tuberculous lymphadenopathy: MR imaging findings. Abdom Imaging 25:627–32
46. Horton KM, Corl FM, Fishman EK (1999) CT of nonneoplastic diseases of the small bowel: spectrum of disease. J Comput Assist Tomogr 23:417–428
47. Nicolas AI, Ros PR (1995) Marbles in the belly: imaging-pathologic correlation of solid mesenteric/omental masses. Postgrad Radiol 15:51–73
48. Jadvar H, Mindelzun RE, Olcott EW, Levitt DB.1997) Still the great mimicker: abdominal tuberculosis. AJR Am J Roentgenol 168:1455–1460
49. Hulnick DH, Megibow AJ, Naidich DP, Hilton S, Cho KC, Balthazar EJ (1985) Abdominal tuberculosis: CT evaluation. Radiology 157:199–204
50. Demir K, Okten A, Kaymakoglu S, Dincer D, Besisik F, Cevikbas U, Ozdil S, Bostas G, Mungan Z, Cakaloglu Y (2001) Tuberculous peritonitis–reports of 26 cases, detailing diagnostic and therapeutic problems. Eur J Gastroenterol Hepatol 13: 581–585
51. Yilmaz T, Sever A, Gur S, Killi RM, Elmas N (2002) CT findings of abdominal tuberculosis in 12 patients. Comput Med Imaging Graph 26:321–325
52. Ha HK, Jung JI, Lee MS, Choi BG, Lee MG, Kim YH, Kim PN, Auh YH (1996) CT differentiation of tuberculous peritonitis and peritoneal carcinomatosis. AJR Am J Roentgenol 167: 743–748
53. Jelinek JS, Kransdorf MJ, Shmookler BM, Aboulafia AJ, Malawer MM (1993) Liposarcoma of the extremities: MR and CT findings in the histologic subtypes. Radiology 186:455–459

54. Kim T, Murakami T, Oi H, Tsuda K, Matsushita M, Tomoda K, Fukuda H, Nakamura H (1996) CT and MR imaging of abdominal liposarcoma. AJR Am J Roentgenol 166:829–833
55. Munk PL, Lee MJ, Poon PY, Goddard KJ, Knowling MA, Hassell PR (1996) Computed tomography of retroperitoneal and mesenteric sarcomas: a pictorial essay. Can Assoc Radiol J 47: 335–341
56. Enzinger FM, Weiss SM (1995) Benign tumors of peripheral nerves. In: Enzinger FM, Weiss SW (eds) Soft tissue tumors. St Louis, Mosby
57. Pui MH, et al (1998) Computed tomography of abdominal neurogenic tumours. Australas Radiol 42(3):183–187
58. Kim SH, Choi BI, Han MC, et al (1992) Retroperitoneal neurilemnoma: CT and MR findings. Am J Roentgenol 159: 1023
59. Cerofolini E, Landi A, DeSantis G, et al (1991) MR of benign peripheral nerve sheath tumors. J Comput Assist Tomogr 15:593
60. Loke TKL, Yuen NWF, Lo KKL, et al (1998) Retroperitoneal ancient schwannoma: Review of clinico-radiological features. Australas Radiol 42(2):136–138
61. Suh JS, Abenoza P, Galloway HR, et al (1992) Peripheral (extracranial) nerve tumors: correlation of MR imaging and histologic findings. Radiology 183:341
62. Varma DG, Moulopoulos A, Sara AS, et al (1992) MR imaging of extracranial nerve sheath tumors. J Comput Assist Tomogr 16:448
63. Friedman DP, Tartaglino LM, Flanders AE (1992) Intradural schwannomas of the spine: MR findings with emphasis on contrast-enhancement characteristics. Am J Roentgenol 158:1347
64. Ros PR, Yuschok TJ, Buck JL, et al (1991) Peritoneal mesothelioma: radiologic appearances correlated with histology. Acta Radiol 32:355–358
65. O'Brien JE, Stout AP (1964) Malignant fibrous xanthomas. Cancer 17:1445–58
66. Enzinger FM, Weiss SW (1995) Malignant fibrohistiocytic tumors. In: Enzinger FM, Weiss SW (eds) Soft tissue tumors. St Louis, MO: Mosby Year Book, pp 351–380
67. Weiss SW, Enzinger FM (1978) Malignant fibrous histiocytoma: an analysis of 200 cases. Cancer 41:2250–2266
68. Goldman SM, Hartman DS, Weiss SW (1986) The varied radiographic manifestations of retroperitoneal malignant fibrous histiocytoma revealed through 27 cases. J Urol 135: 33–38
69. Ros PR, Viamonte M Jr, Rywlin AM (1984) Malignant fibrous histiocytoma; mesenchymal tumor of ubiquitous origin. AJR 142:753–759
70. Bruneton JN, Drouillard J, Rogopoulos A, Laurent F, Normand F, Balu-Maestro C, et al (1988) Extraretroperitoneal abdominal malignant fibrous histiocytoma. Gastrointest Radiol 13:299–305
71. Ko SF, Wan YL, Lee TY, Ng SH, Lin JW, Chen WJ (1998) CT features of calcifications in abdominal malignant fibrous histiocytoma. Clin Imaging 22:408–13
72. Castillo M, Davis PC, Takei YD, Schwartzberg DG, Hoffman JC Jr (1990) Intracranial cystic malignant fibrous histiocytoma in a child: sonographic and CT findings. Pediatr Radiol 20:194–5
73. Berry AD III, Reintjes SL, Kepes JJ (1988) Intracranial malignant fibrous histiocytoma with abscess-like tumor necrosis. J Neurosurg 69:780–784
74. Panicek DM, Casper ES, Brennan MF, Hajdu SI, Heelan RT (1991) Hemorrhage simulating tumor growth in malignant fibrous histiocytoma at MR imaging. Radiology 181:398–400
75. Munk PL, Sallomi DF, Janzen DL, et al (1998) Malignant fibrous histiocytoma of soft tissue imaging with emphasis on MRI. J Comput Assist Tomogr 22:819–826
76. Fenoglio-Preiser CM, Pascal RR, Perzin KH (1990) Mesenchymal tumors. In: Leiomyosarcomas; tumors of the intestines. 2nd series. Washington, DC: Armed Forces Institute of Pathology, 433–441
77. Arakawa A, Yasunaga T, Yano S, et al (1993) Radiological findings of the retroperitoneal leiomyosarcoma: report of two cases. Comput Med Imaging Graph 17:125
78. Hartman DS, Hayes WS, Choyke PL, et al (1992) From the archives of the AFIP: leiomyosarcoma of the retroperitoneum and inferior vena cava: radiologic-pathologic correlation. Radiographics 12:1203
79. Lane RH, Stephens DH, and Reiman HM (1989) Primary retroperitoneal neoplasms: CT findings in 90 cases with clinical and pathologic correlation. Am J Roentgenol 152: 83
80. Maya MM, Fried K, Gendal ES (1993) AIDS-related lymphoma: an unusual cause of omental caking. AJR Am J Roentgenol 160:661
81. Pantongrag-Brown L, Buetow PC, Carr NJ, Lichtenstein JE, Buck JL (1995) Calcification and fibrosis in mesenteric carcinoid tumor: CT findings and pathologic correlation. AJR Am J Roentgenol 164:387–391
82. Einstein DM, et al (1991) Abdominal lymphadenopathy: spectrum of CT findings. Radiographics 11: 457
83. Kim Y, Cho O, Song S, Lee H, Rhim H, Koh B (1998) Peritoneal lymphomatosis: CT findings. Abdom Imaging 23:87–90
84. Bader TR, Semelka RC, Chiu VC, Armao DM, Woosley JT (2001) MRI of carcinoid tumors: spectrum of appearances in the gastrointestinal tract and liver. J Magn Reson Imaging 14: 261–269
85. Emory TS, Carr NJ, Sobin LH (1997) Sclerosing mesenteritis, mesenteric panniculitis and mesenteric lipodystrophy: a single entity? Am J Surg Pathol 21:392–398
86. Katz ME, Heiken JP, Glazer HS, Lee JKT (1985) Intraabdominal panniculitis: clinical, radiographic, and CT features. AJR 145:293–296
87. Mata JM, Inaraja L, Martin J, et al (1987) CT features of mesenteric panniculitis. J Comput Asst Tomogr 11:1021–1023
88. Lawler LP, McCarthy DM, Fishman EK, Hruban R (2002) Sclerosing mesenteritis: depiction by multidetector CT and three-dimensional volume rendering. AJR Am J Roentgenol 178:97–99
89. Kronthal AJ, Kang YS, Fishman EK, Jones B, Kuhlman JE, Tempany CM (1991) MR imaging in sclerosing mesenteritis. AJR Am J Roentgenol 156:517–519
90. Kakitsubata Y, Umemura Y, Kakitsubata S, Tamura S, Watanabe K, Abe Y, Hatakeyama K (1993) CT and MRI manifestations of intraabdominal panniculitis. Clin Imaging 17: 186–188
91. Fujiyoshi F, Ichinari N, Kajiya Y, Nishida H, Shimura T, Nakajo M, Matsunaga Y, Furoi A, Imaguma M (1997) Retractile mesenteritis: small-bowel radiography, CT, and MR imaging. AJR Am J Roentgenol 169:791–793
92. Dalen BP, Bergh PM, Gunterberg BU (2003) Desmoid tumors: a clinical review of 30 patients with more than 20 years' follow-up. Acta Orthop Scand 74:455–459
93. Middleton SB, Clark SK, Matravers P, Katz D, Reznek R, Phillips RK (2003) Stepwise progression of familial adenomatous polyposis-associated desmoid precursor lesions demonstrated by a novel CT scoring system. Dis Colon Rectum 46: 481–485
94. Al Jadaan SA, Al Rabeeah A (1999) Mesenteric fibromatosis: case report and literature review. J Pediatr Surg 34:1130–1132
95. Tolg C, Poon R, Fodde R, Turley EA, Alman BA (2003) Genetic deletion of receptor for hyaluronan-mediated motility (Rhamm) attenuates the formation of aggressive fibromatosis (desmoid tumor). Oncogene 22:6873–6882
96. Maconi G, Cristaldi M, Vago L, Rovati M, Elli M, Sampietro GM, Nebuloni E, Sainaghi M, Taschieri AM, Bianchi Porro G (1998) Clinical, ultrasonographic and tomographic features on the natural evolution of primary mesenteric fibromatosis: a case report. Hepatogastroenterology 45:1663–1666
97. Kawashima A, Goldman SM, Fishman EK, Kuhlman JE, Onitsuka H, Fukuya T, Masuda K (1994) CT of intraabdominal desmoid tumors: is the tumor different in patients with Gardner's disease? AJR Am J Roentgenol 162:339–342
98. Quinn SF, Erickson SJ, Dee PM, et al (1991) MR imaging in fibromatosis: results in 26 patients with pathologic correlation. AJR 156:539–542
99. Healy JC, Reznek RH, Clark SK, Phillips RK, Armstrong P (1997) MR appearances of desmoid tumors in familial adenomatous polyposis. AJR Am J Roentgenol 169:465–472

100. Castleman B, Iverson L, Mercedez VP (1956) Localized mediastinal lymph node hyperplasia resembling thymoma. Cancer 9:822–830
101. Keller AR, Hochholzer L, Castleman B (1976) Hyaline vascular and plasma-cell types of giant lymph node hyperplasia of the mediastinum and other locations. Cancer 29:670–681
102. Kim TJ, Han JK, Kim YH, Kim TK, Choi BI (2001) Castleman disease of the abdomen: imaging spectrum and clinicopathologic correlations. J Comput Assist Tomogr 25:207–214
103. Meador TL, McLarney JK (2000) CT features of Castleman disease of the abdomen and pelvis. AJR Am J Roentgenol 175:115–118
104. Singletary LA, Karcnik TJ, Abujudeh H (2000) Hyaline vascular-type Castleman disease: a rare cause of a hypervascular retroperitoneal mass. Abdom Imaging 25:207–209
105. Irsutti M, Paul JL, Selves J, Railhac JJ (1999) Castleman disease: CT and MR imaging features of a retroperitoneal location in association with paraneoplastic pemphigus. Eur Radiol 9:1219–1221
106. Johnson WK, Ros PR, Powers C, Stoupis C, Segel KH (1994) Castleman disease mimicking an aggressive retroperitoneal neoplasm. Abdom Imaging 19:342–344
107. Livingston CD, Levine BA, Lecklitner ML, Sirinek KR (1983) Incidence and function of residual splenic tissue following splenectomy for trauma in adults. Arch Surg 118:617–620
108. Katz DS, Moshiri M, Smith G, Meiner EM, Fruauff AA (1998) Spontaneous hemorrhage of abdominal splenosis. J Comput Assist Tomogr 22:725–727
109. Carr NJ, Turk EP (1992) The histological features of splenosis. Histopathology 21:549–553
110. Delamarre J, Capron JP, Drouard F, Joly JP, Deschepper B, Carton S (1988) Splenosis: ultrasound and CT findings in a case complicated by an intraperitoneal implant traumatic hematoma. Gastrointest Radiol 13:275–278
111. Lin WC, Lee RC, Chiang JH, Wei CJ, Chu LS, Liu RS, Chang CY (2003) MR features of abdominal splenosis. AJR Am J Roentgenol 180:493–496
112. Castellani M, Cappellini MD, Cappelletti M, Fedriga E, Reschini E, Cerino M, Gerundini P (2001) Tc-99m sulphur colloid scintigraphy in the assessment of residual splenic tissue after splenectomy. Clin Radiol 56:596–598